MAY 1979 PPPL-1551
UC-20f

VACUUM SYSTEM DESIGN AND TRITIUM INVENTORY FOR THE TFTR CHARGE EXCHANGE DIAGNOSTIC

BY

S. S. MEDLEY

PLASMA PHYSICS LABORATORY

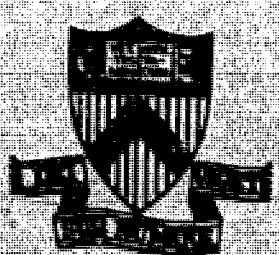

PRINCETON UNIVERSITY
PRINCETON, NEW JERSEY

This work was supported by the U. S. Department of Energy Contract No. EY-76-C-02-3073. Reproduction, translation, publication, use and disposal, in whole or in part, by or for the United States Government is permitted.

VACUUM SYSTEM DESIGN AND TRITIUM INVENTORY FOR THE TFTR CHARGE EXCHANGE DIAGNOSTIC

by

S. S. Medley

ABSTRACT

The charge exchange diagnostic for the TFTR is comprised of two analyzer systems which contain a total of twenty independent mass/energy analyzers and one diagnostic neutral beam tentatively rated at 80 keV, 15 A. The associated vacuum systems were analyzed using the Vacuum System Transient Simulator (VSTS) computer program which models the transient transport of multi-gas species through complex networks of ducts, valves, traps, vacuum pumps, and other related vacuum system components. In addition to providing improved design performance at reduced cost, the analysis yields estimates for the exchange of tritium from the torus to the diagnostic components and of the diagnostic working gases to the torus.

I. INTRODUCTION

The charge exchange neutral analyzer (CENA) diagnostic for TFTR provides two autonomous analyzer systems and one shared diagnostic neutral beam (DNB). Although some degree of functional overlap exists, one analyzer system is dedicated to measurement of the perpendicular thermalized ion energy distribution (ion temperature) while the other primarily yields the slowing-down energy distribution of beam injected ions. The perpendicular system views from the basement level along 12 parallel vertical chords which are spaced roughly equidistantly across a minor diameter of the torus, as shown in Fig. 1. The tangential system is located in the test cell at Bay Q. As illustrated in Fig. 2, the analyzers view a fan-like array of chords in the equitorial plane which encompasses a wide range of angles with respect to the toroidal field direction. The steerable diagnostic neutral beam mounted at Bay A provides a temporally-modulated, spatially-localized enhancement of the charge exchange efflux in the viewing field of both analyzer systems, though in general not concurrently.

Each charge exchange line-of-sight is provided with an identical but independent CENA module. An analyzer module consists basically of a gas stripping cell, a region of superimposed, parallel electric and magnetic fields for mass/energy analysis, and a channel electron multiplier array detector. These components are contained in a magnetically shielded enclosure which is evacuated by a turbo-molecular pump. Each module has a direct view of the plasma through an evacuated flight tube.

The basic performance requirements of the vacuum system are as follows. Under a gas load (typically helium) of 1-5 m Torr·ℓ/sec due to the stripping cell, the analyzer enclosure and the flight tube should be maintained in the low 10^{-6} Torr pressure range or less. The quantity of gas from the analyzers which can be

permitted to enter the torus is somewhat debatable. For TFTR, a design goal of 10^{-4} Torr·ℓ/sec from the whole analyzer system has been adopted, which corresponds to a torus partial pressure of $\sim 10^{-9}$ Torr due to analyzer working gas. During tritium operation, the partial pressure of tritium in the analyzer must be below 10^{-8} Torr in order for the tritium-induced background detector count rate to be negligible. Tritium accumulation in the analyzer during extended operation must also be considered, though at the present time only crude estimates exist for the level of tritium build-up that can be tolerated. In the event that the total level should restrict operation of the diagnostic, provision will be made to periodically reduce the accumulation of tritium using vacuum bakeout procedures.

The vacuum requirements for the diagnostic neutral beam differ in several respects from those of the analyzer system. A schematic showing the major components for the tentative diagnostic neutral beam design is given in Fig. 3. First, the neutral source working gas is either H_2 or D_2 with a feed rate of 5-10 Torr·ℓ/sec. In order to maintain most of the beamline in the low 10^{-5} Torr pressure range in the presence of this massive gas load, it is necessary to employ large-area helium cryogenic pumping. The allowable exchange of source working gas between the beamline and the torus is less stringent in this case because in general the neutral beam and plasma working gases are compatible. As a guideline, it is required that the beamline contribute 1% or less to the plasma density at $n_e = 1 \times 10^{13} cm^{-3}$. This implies a gas flow from the beamline to the torus of the order of 1 Torr·ℓ/sec or less. Similarly, a flow rate of the order of 1 Torr·ℓ/sec of tritium into the beamline from the torus is acceptable since the beamline does not contain equipment which is sensitive to tritium contamination. However, the throughput of tritium in the beamline should be minimized in the interest of reducing the tritium handling aspects of the beamline vacuum system.

The vacuum requirements outlined above were analyzed using the VSTS computer program for the purpose of optimizing the system performance, minimizing the cost of the vacuum equipment and examining the tritium handling problems for the charge exchange diagnostic apparatus.

II. THE VACUUM SYSTEM TRANSIENT SIMULATOR CODE

The Vacuum System Transient Simulator (VSTS) code was engineered and programmed by J. Sredniawski of Grumman Aerospace Corporation specifically for the design of the main torus vacuum system of the Tokamak Fusion Test Reactor (TFTR) at PPPL. A complete description of the vacuum modeling techniques and the code methodology is available in an engineering report.[1] In order to operate the program at PPPL, the code as written for the IBM-based Grumman Calldata™ computer system was reprogrammed on the PPLCC CYBER facility by Herb Fishman. A new user manual[2] for the CYBER version of the VSTS code is in preparation.

The VSTS computer program models the transient gas transport through complex networks of ducts, valves, traps, vacuum pumps, and other associated vacuum system components. The code is capable of modeling simultaneously a mixture of up to 10 gas species through continuum, transition, and molecular flow regimes. Although developed specifically for the TFTR torus vacuum system design, the VSTS is a generalized program capable of handling a broad range of vacuum system applications.

In the VSTS methodology, a vacuum system network is modeled as a matrix of pressure nodes. The nodes are usually beginning and end points for system components, which means that the connection between two nodes is represented by the characteristic performance of a type of component. Components (or connections) may be pumps (mechanical, turbomolecular, cryogenic), ducts of cylindrical or

rectangular geometry, valves, baffles, or specific gas load sources. Also provision exists to assign distributed outgassing for any vacuum surface,and bakeout procedures can be simulated. Each type of connection or process is modeled by a particular subroutine in VSTS. As nodes are established and connected from the input data, their volumes and surface areas are determined based upon connection geometry. Both the volume and surface area of each connection are split equally and concentrated at each of the two end-point nodes. The final result is a matrix model where each pressure node contains a summation of all the half-volumes and half-surface areas of the adjacent components.

The numerical finite difference technique is used in VSTS to model the transient performance. A user-specified initial matrix of nodal pressures is used to start the calculation. The individual connection throughputs are then determined by the applicable connection subroutine model using the connection geometry and nodal pressure difference. For each node, the throughputs into and out of that node are algebraically summed to give a net throughput. Once all net throughputs have been determined, the entire nodal pressure matrix is updated for a small increment in time. The updated pressure matrix is used once again to determine new throughputs. The process is iterated over small time differences to model the actual transient.

The VSTS software is actually a group of three FORTRAN IV programs that can operate independently or in sequence. The first FORTRAN program (VSTS1) handles data input, the second (VSTS2) executes the transient performance, and the third (VSTS3) performs graphic plotting. These programs are interfaced by common data sets and job control routines as required by the specific computer on which the code is programmed. All programs are written in FORTRAN IV and hence the major aspects of the code operation as previously documented[1] apply to the version on the PPLCC CYBER system. However, the job control format as well as certain aspects of the input/output format have been modified for the CYBER version.[2]

The VSTS1 program operates in an interactive time-sharing mode and cues the user with a series of preprogrammed dialogue for the purpose of generating the input data sets required to model a given vacuum system. An intial input data set may be subsequently modified or expanded while preserving the remainder of the data set by either re-calling the VSTS1 routine or using the computer system file editor. This modification capability enables extensive revision of the vacuum system as desired while minimizing tedious duplication of the data input for individual vacuum components. The resulting data sets are then used in the VSTS2 program which executes in a non-interactive time-sharing mode all of the calculations to model the performance of a given vacuum system. The VSTS2 performance data are output in three forms, any of which can be specified as an option by the user. One form is a standard printed output which includes all of the detailed parameters such as geometry, gas properties, nodal pressures, and conductances throughout the model network. The second form of output is the generation as part of the execution of VSTS2 of plots of pressures and gas throughputs versus time for user selected nodes and connections throughout the vacuum network. The third form of output is the generation of pressure and throughput tables for user specified nodes and connections. These tables may be simply printed out or may be used subsequently by the VSTS3 program for interactive graphics plotting.

In addition to the subroutines for modeling the various vacuum components, VSTS2 contains a preprogrammed subroutine to simulate the pulsed plasma discharge for TFTR which may be invoked at the option of the user. During non-pulsed operation the torus is treated like any other component of the vacuum model. However, during pulsed mode operation, a working gas (H_2, D_2, T_2) is injected into the torus and subsequently compressed toward the torus centerline by the plasma discharge. When the gas is compressed and contained, the plasma periphery sees a much lower molecular density. At the same time, the energy level of the particles

that diffuse out of the contained plasma and occupy the plasma/wall interface region is significantly higher than that in the absence of the discharge. This results in an increased equivalent temperature for the interface region.

As an aid to determining vacuum system performance during the short period of a plasma discharge, a forcing function routine was set up in VSTS2. The routine imposes a pressure and temperature profile in the torus that is representative of the conditions in the interface region during a pulse. Figure 4 shows a typical pulse scenario. Gas must be initially injected by some other subsystem or by means of a puffer jet. This phase is called the "prefill." The pressure at the end of the prefill and before a pulse is initiated must be greater than the pressure during the "containment" phase. The pressure during containment is presently set at 2×10^{-6} Torr (room temperature equivalent) based upon current estimates of TFTR performance by PPPL physicists. After prefill has been achieved, the pulse routine is executed. When the pulse is executed, the partial pressures of all species are reduced proportionally in 10 msec such that a total pressure of 2×10^{-6} Torr is achieved. This is the compression phase during which the temperature is raised to $113000^{o}K$ (10 ev). The containment is then held for an expected period of 750 msec while additional working gases may be introduced into the torus. An inventory is continually kept up to date on the amount of gas injected so that, when the containment is terminated, proper pressure is achieved after expansion. The expansion phase takes an estimated 100 msec, during which the temperature is reduced to $293^{o}K$ and the final total pressure is determined from PVT relationships.

In view of the complexity of the VSTS computer program, it is impractical to describe in detail the setting-up of the charge exchange vacuum system models used in this report. However, sufficient detail is presented to specify the geometrical and functional characteristics of all components in each vacuum system.

III. GENERAL CHARACTERISTICS OF THE MODEL FOR THE CHARGE EXCHANGE VACUUM SYSTEMS

As a simple beginning, one arm of the perpendicular charge exchange system will be modeled. An arm consists of an analyzer module connected to the TFTR torus through a flight tube interrupted by an intermediary pumping plenum, as illustrated in Fig. 1. The mechanical layout of the vacuum system for a single arm is shown in Fig. 5. The torus is provided with a gas feed (or puffer) and a single pump which simulates the net pumping characteristics of the actual torus pumping system. From the torus, a flight tube connects the arm to an intermediary (or fore) plenum, whose function is to provide a pumping station for evacuation of the long flight tube. A valve in the flight tube is inserted just before the plenum to isolate the torus and analyzer vacuum systems. Another length of valved flight tube connects the fore plenum to the analyzer module. Both the fore plenum and analyzer module are evacuated with a dedicated turbomolecular pump backed by a mechanical pump. Valved ducts provide the relevant interconnections. The analyzer module has a gas feed to simulate the stripping cell gas source.

The nodal network associated with this vacuum system is shown in Fig. 6. Parameters given below for the network components are characteristic, though in the course of the analysis certain of them were modified as will be noted later.

The TFTR torus is modeled as a node (1) having a calculated volume of 1.0×10^8 cm^3 and surface area of 9.2×10^6 cm^2 which is evacuated by an idealized pump of speed 8000 ℓ/sec for nitrogen. A gas feed introduces tritium to the torus at a rate of 100 Torr·ℓ/sec. The flight tube has a uniform inside diameter of 5.72 cm and nodal points (2,3,8) are distributed along its length to enable pressure determination at approximately one meter intervals. Actuated gate valves of the same internal diameter as the flight tube are located near the entrance of both the fore plenum and analyzer module. The actuating (opening/closing) time of any valve

in the system can be specified by the user. The fore plenum is treated as a node (4) of volume 1.9×10^5 cm^3 and surface area 2.3×10^4 cm^2 corresponding to a cylinder of approximately 200 cm in length and 35 cm in diameter. A Leybold-Heraeus* 1500 ℓ/sec turbomolecular pump evacuates the fore plenum through a 50 cm long, 25 cm diameter valved duct which is connected to a Leybold-Heraeus 12 ℓ/s D60A roughing pump by a 100 cm long, 7.6 cm diameter valved duct (5,6,7,14). Nominal inside dimensions of the analyzer enclosure are 18 x 70 x 80 cm and this component was modeled as a node (9) of volume 1.0×10^5 cm^2 and surface area 1.7×10^4 cm^2. The pumping system for the analyzer is identical to that for the fore plenum except the diameter of the analyzer-turbomolecular connecting duct was reduced to 15.2 cm due to the constraint imposed by the 18 cm inside width of the analyzer enclosure (10,11,12,14). Finally, the analyzer stripping cell is simulated by a He gas feed of selectable leak rate. The VSTS modeling methodology, consecutive integers are assigned to nodal points starting with (1) for the torus and ending with a common node, here (14), for all connections between the vacuum system and atmospheric pressure.

To establish the baseline performance of the vacuum system model, the torus was filled with N_2, T_2, D_2, He and H_2 gas species each at a partial pressure of 1×10^{-3} Torr and pumpdown to base pressure was calculated with all systems operating. The results shown in Fig. 7 give the total pressure as a function of time with the curve index numbers designating the nodal points in Fig. 6 corresponding to each pressure curve. In explanation, within a few seconds a quasi-equilibrium pressure distribution is established throughout the system, the analyzer pressure being lowest at approximately 2×10^{-6} Torr. Thereafter pumpdown of the entire system parallels the rate set by the torus vacuum system until the base pressures of

*Throughout this report, the use of brand names does not constitute a recommendation either for or against the use of these products.

the various nodal points are reached. The base pressures are determined by the net pumping speed at a given node combined with the outgassing rate[1] of the nodal area assigned by the user for each gas component. The performance of the torus vacuum system used in this model provides an acceptable simulation of the actual TFTR system (see Ref. 1, page 6-5).

Prior to analysis of the full charge exchange vacuum system, aspects of the design were examined with the single arm model using the following vacuum conditions and sequence of events. At an initial partial pressure of 1×10^{-9} Torr for T_2 and 1×10^{-11} Torr for He throughout the system, all valves were opened and all vacuum pumps turned on. Helium injection at a leak rate of 0.002 Torr·ℓ/sec into the analyzer module commenced at 2.0 sec and continued for 5.0 sec to simulate pulsed operation of the stripping cell. Tritium injection at a rate of 100 Torr·ℓ/sec into the torus started at 3.0 sec. At 4.0 sec, tritium injection ceased and simultaneously the fore plenum valve was closed (closure time, 1.5 sec) to isolate the torus and analyzer vacuum systems. The calculation ended shortly after the analyzer system had pumped down to base pressure (10.0 sec).

The computed transient partial pressure distribution throughout the model corresponding to this sequence of events is shown in Fig. 8. In the figure, the numbers appended to the curves identify the nodal points in Fig. 6 to which each pressure curve applies. As can be seen, at the end of T_2 injection, the torus pressure equilibrates at $\sim 10^{-3}$ Torr (curve 1). Beyond the fore plenum isolation valve, the tritium pressure has not equilibrated, but a peak pressure of $\sim 4.0 \times 10^{-7}$ Torr is reached in the analyzer (curve 9) partway through closure of the isolation valve. In Fig. 8B, the helium partial pressure in the analyzer equilibrates in ~ 0.5 sec at a pressure of 3.0×10^{-6} Torr (curve 9). The increase of He pressure in the torus (curve 1) reflects the fact that the calculation was initialized at a pressure of 1.0×10^{-11} Torr, which is below the base pressure of $\sim 10^{-10}$ Torr determined by the outgassing rate for He as well as the torus area and pumping speed.

Using the data from Fig. 8, the peak pressures measured at t = 5.0 sec are plotted in Fig. 9 as a function of the distance of the various nodal points from the torus node. Curves B show the tritium (upper) and helium (lower) partial pressure distributions for the case described above. Curves A show the corresponding data obtained with the fore plenum and its associated vacuum pumps removed. Clearly, the pumped plenum is effective in reducing the pressures along the flight tube and consequently the exchange of working gases between the torus and analyzer module. Curves C show the effect on the pumped plenum case of introducing a conductance restriction at the entrance of the flight tube to the analyzer module. The conductance of a tube is proportional to the product of the cross sectional area of the tube bore and ratio of the bore diameter to tube length (which ratio determines the probability of transmission of a gas molecule in the molecular flow regime). Thus restricting the conductance of a tube is, in practice, more effectively accomplished by reducing its diameter rather than increasing its length. However, a lower limit is imposed on the diameter reduction by the requirement not to obscure the viewing field of the analyzer. A compromise conductance restriction having diameter 0.5 cm and length 15.0 cm was used in obtaining the results shown by curves C. As a result of introducing this restriction, the tritium pressure in the analyzer and the helium pressure in the flight tube were reduced by two orders of magnitude or more at the expense of a much smaller increase in tritium pressure in the length of flight tube between the fore plenum and the analyzer module. Introducing an additional restriction at the entrance to the fore plenum on the torus side was determined to be relatively ineffective, since the viewing field of the analyzer at this location does not permit a significant reduction in the diameter of the flight tube.

As will be discussed further in the next section, the VSTS code also provides the gas flow (Torr·ℓ/sec) for each species through any user-specified connections (i.e., between adjoining nodal points). The time integrated gas flow, of course, gives the

total quantity of gas (Torr·ℓ) through the specified connection for a given gas species. In this manner, the quantity of tritium through the analyzer turbomolecular pump for case C of Fig. 9 was determined to be 30 μCi. If the flight tube valve at the analyzer entrance is closed simultaneously with the fore plenum valve, the tritium pumped through the analyzer is reduced to 1.7 μCi.

The analyzer pumping arrangement was modified to examine the performance of a larger pump shared between several analyzers. Three analyzer modules were connected to a common plenum, the optional plenum shown in Fig. 6, and the plenum was pumped by one 3500 ℓ/s Leybold-Heraeus turbomolecular pump backed by a DK200 roughing pump. All ducts were suitably scaled in dimensions so as not to restrict the increased pumping speed. The performance of this arrangement was essentially identical (±10%) to the results shown by curve C in Fig. 9. Therefore, individual 1500 ℓ/s pumps or one 3500 ℓ/s pump connected to three analyzer modules via a common plenum give essentially equivalent performance.

The information obtained through the above investigations is utilized in modeling the complete perpendicular analyzer system described in the next section.

IV. ANALYSIS OF THE PERPENDICULAR CHARGE EXCHANGE VACUUM SYSTEM

The vacuum system for the full perpendicular charge exchange system consisting of twelve analyzer modules connected individually by flight tubes to the torus through a common pumped plenum (see Fig. 1) is modeled in this section. The nodal network for this vacuum system shown in Fig. 10 can be described by considering one arm (nodes 1-14 plus the ambient node 70) since the remaining eleven arms are identical except for one minor aspect which will be discussed momentarily. The flight tube connecting the torus to the fore plenum is provided with several nodal points (1-5) for the purpose of determining the pressure distribution along its length. The fore plenum has the same isolation valve and pumping system as described in the

previous section. A 0.5 cm diameter, 15.0 cm long conductance restriction is combined with a valve in the section of flight tube connecting the fore plenum to the analyzer module (nodes 5, 9, 10, 11). The analyzer pumping arrangement and helium gas feed are as described earlier. For the remaining arms, the number of flight tube nodal points is reduced and the backing pumps were connected directly to the analyzer turbomolecular pumps. The tritium gas feed rate to the torus is 100 Torr·ℓ/sec as before and each analyzer module is provided with a 0.002 Torr·ℓ/sec helium gas feed.

Fig. 11 shows the transient T_2 and He partial pressure curves for the noted nodal points corresponding to the following sequence of events. After opening all valves and starting all pumps, helium was injected into each analyzer module, starting at 0.5 sec and ending at 2.5 sec (Fig. 11B). Tritium injection into the torus commenced at 1.0 sec (Fig. 11A). In this calculation, the plasma discharge is simulated as described in Section II. Following the torus node (curve 1 in Fig. 11A), the plasma discharge is initiated at 1.2 sec. Due to the discharge, the tritium partial pressure at the plasma edge drops sharply to 2.0×10^{-6} Torr. The plasma pulse terminates at 1.95 sec, after which the torus tritium pressure rises to $\sim 1.0 \times 10^{-3}$ Torr. This pressure results from the cumulated inventory of tritium which was injected at a constant rate throughout the duration of the plasma pulse. At 2.0 sec, all fore plenum valves were closed (closure time of 0.5 sec) and at 2.5 sec helium injection was terminated. All analyzer flight tube valves remained open, with the exception of the valve between nodes 16 and 17. The accelerated pumpout of tritium in the associated analyzer module due to closure of this valve is shown by curve 17 in Fig. 11A.

Several features of the tritium and helium transient pressure curves merit comment. Looking first at the tritium partial pressure curves, it is important to note that during the plasma discharge, the tritium pressure increase in the analyzer

module is greatly reduced compared with that due to simply puffing the same quantity of tritium into the torus, as shown in curve 9 of Fig. 8A. This reduction, of course, results from the drop in plasma edge pressure caused by the discharge. Even after the analyzer measurement period during the discharge, the tritium pressure rises only slightly above the design goal of 1.0×10^{-8} Torr. Turning to the He partial pressure curves, it can be seen that the helium pressure throughout the network is sensibly constant during the discharge and the analyzer pressure at 3×10^{-6} Torr (curve 11) is within the design goal range.

The distribution of T_2 and He partial pressures from the torus to the analyzers corresponding to a time of 1.9 sec in Fig. 11 are plotted in Fig. 12. The heavy solid and broken curves represent the model discussed above while the lighter curves represent the same model, except the 1500 ℓ/s turbomolecular pumps on the analyzers were replaced by 500 ℓ/s Leyboid-Heraeus pumps backed by D60A mechanical roughing pumps, the pumping arrangement on the fore plenum being unchanged. In both cases, the tritium and helium pressure distributions are essentially the same with the helium pressures being an order of magnitude or more below the design goal (Section I) throughout 98% of the flight tube. However, with the 500 ℓ/s pumps, the helium pressure in the analyzer is $\sim 7.0 \times 10^{-6}$ Torr which is approaching the acceptable operation limit.

Other calculations were carried out in which the helium flow rate to the analyzer modules was increased from 0.002 to 0.1 Torr·ℓ/sec. Over this range, the increase in helium pressure within the analyzer was directly proportional to the change in He flow rate for both the 500 ℓ/s and 1500 ℓ/s analyzer pumping arrangements. The possibility of reducing the analyzer He pressure through appropriate design of the stripping cell will be considered later in this section.

The transient gas flow (Torr·ℓ/sec) through selected vacuum system components is presented for tritium in Fig. 13A and for helium in Fig. 13B for the

sequence of events pertaining to Fig. 11. The area under each curve gives the quantity of gas passed through the associated vacuum component. Table I presents a tabulation of this quantity in units of Torr·ℓ for each curve, as well as in units of Curies (1 Torr·ℓ $\cong$ 3.4 Curie) for the tritium curves. Two points are noteworthy concerning the required performance of the vacuum system. First of all, for a torus tritium gas load of 340 Curies, the amount of tritium passed through each analyzer module per machine pulse is 22 μCi with closure of the analyzer flight tube valve (44 μCi without this closure). Secondly, of the 0.004 Torr·ℓ helium injected into each analyzer, $\sim 1.0 \times 10^{-6}$ Torr passes through the flight tube into the torus. This flow for 12 analyzers into a torus volume of 1.0×10^{8} cm^3 amounts to a helium pressure in the torus of $\sim 1.2 \times 10^{-10}$ Torr which is comparable to the base torus partial pressure of helium for the model. On the basis of a single discharge, therefore, the exchange of working gases between the torus and analyzers is very small. However, the tritium build-up in the analyzers due to partial retention of the tritium throughput over a large number ($\sim$ 4000) of discharges might still pose a problem.[3] In the absence of reliable numbers to determine the tritium accumulation, the following ad hoc estimate is offered. If 1% of the 6.5 Torr·ℓ of tritium is retained in the analyzer, for 4000 discharges, then the accumulated tritium would result in an equivalent pressure of 2.6×10^{-7} Torr if it occupied the 1.0×10^{5} cm^3 volume of the analyzer module. This pressure is approximately two orders of magnitude above the design level of $\sim 10^{-9}$ Torr. Although this accumulated pressure equivalent is probably greatly overestimated, it indicates that the problem of tritium retention in the analyzers deserves further analysis.

TABLE I

QUANTITY OF T_2 AND He TRANSFERRED THROUGH SELECTED COMPONENTS OF THE PERPENDICULAR CHARGE EXCHANGE VACUUM MODEL

Gas Species	Component	Torr·ℓ	Curies
T_2	Torus Gas Feed	100	340
	Fore Plenum Pump	0.054	0.18
	Analyzer*	1.3×10^{-5}	4.4×10^{-6}
He	Cell Gas Feed*	0.004	—
	Fore Plenum Pump	1.3×10^{-5}	—
	Torus*	1.0×10^{-6}	—

*For each analyzer module.

With the exception of the tritium retention problem discussed above, the design of the perpendicular charge exchange analyzer vacuum system meets all the design requirements set forth in Section I provided 1500 ℓ/s turbomolecular pumps are designated for each analyzer module. As mentioned earlier, 500 ℓ/s pumps might suffice if the stripping cell is designed so as to reduce the gas flow into the analyzer while maintaining the required helium pressure ($\geq 10^{-3}$ Torr) inside the cell. A proposed design of the stripping to accomplish this is discussed below.

The mechanical layout of the model for the stripping cell is shown in Fig. 14 with the analyzer module and its pumping system being the same as used earlier. Helium is fed into a cylindrical stripping cell and flows into the analyzer module

through identical tubular apertures at each end of the cell. The analyzer and stripping cell pressure transients similar to those shown in Fig. 6A were calculated for various turbomolecular pump and cell aperture arrangements. The salient model results are presented in Fig. 15. For a single aperture 1.0 cm long and 0.3 cm diameter at each end of the cell, curves A and B give the analyzer pressure using 500 and 1500 ℓs turbomolecular pumps, respectively, as a function of helium gas flow rate. Curves C and D show the same calculation for the case where each end of the stripping cell was provided with two 1.0L x 0.3D apertures separated by a distance the order of the cell diameter. Clearly, the analyzer pressure is reduced by the application of more pumping speed, but a larger (and more cost effective) reduction can be obtained by using multiple cell apertures. Futhermore, the pressure reduction resulting from the double aperture arrangement exceeds that predicted by straightforward conductance considerations due to the transient effects. This is demonstrated in Fig. 16 where the pressure as a function of time is shown for the analyzer, stripping cell and the region between a pair of cell apertures. As is evident, the various pressure ratios have not equilibrated to the conductance ratio values. At the present time, the pressure variation during a 1 second interval around 4.5 seconds appears acceptable from the viewpoint of general charge exchange diagnostic performance though this situation warrants further analysis for certain charge exchange applications.

V. ANALYSIS OF THE TANGENTIAL CHARGE EXCHANGE VACUUM SYSTEM

The vacuum system for the tangential charge exchange system (see Fig. 2) is very similar to that for the perpendicular system. Individual analyzer modules are connected to the torus through flight tubes and an intermediary pumped plenum. However, the geometry of the plenum and the interface between it and the torus are significantly different so that a separate analysis of this system is required.

The nodal network for the tangential system is shown in Fig. 17. Since the VSTS program treats ducts as either cylindrical or rectangular, the pie-shaped plenum sector is modeled in the following rectangular approximation. The plenum sector is divided into two parts of equal "length" as measured along the direction of the central flight tube. Each part is modeled as a rectangular duct of length 100.0 cm and actual design height 15.0 cm. The width of each rectangular section is chosen to produce the same volume as the represented section of the plenum. Between the plenum and the torus, a relatively large-area clear aperture is required to accommodate the viewing field necessary for the analyzer system. As a result, the conductance (and hence gas exchange) between the plenum and torus will be large compared with the perpendicular analyzer system. Details of this aperture section are under design at present. For the purpose of this report, a "worst-case" configuration consisting simply of a large clear-view rectangular aperture is used to generate baseline performance characteristics against which design refinements may be evaluated.

The T_2 and He partial pressure transients for the pulsed discharge mode are given in Fig. 18 for noted nodal points corresponding to the vacuum model of Fig. 17. The sequence of events is the same as for Fig. 11 except that the larger gate valve between the plenum and torus has an increased closure time of 2.5 seconds. As a result, the duration of the tritium pressure rise in the analyzer (curve 10) is extended, but closure of the analyzer valve foreshortens this significantly (curve 15). During the plasma pulse, the He pressure transients are very similar to those observed for the perpendicular charge exchange system (see Fig. 11B). However, the post discharge behavior of the pressure transients reflect the effects of higher conductance and longer valve closing time between the plenum and the torus. The distributions of T_2 and He partial pressures from the torus to the analyzers given in Fig. 19 corresponds to a time of 3.8 seconds in Fig. 18. The helium pressure at the

torus is close to that for the perpendicular system, but the tritium pressure in the analyzer is almost an order of magnitude larger. This higher tritium pressure, which is marginally acceptable for proper analyzer detector performance, is a consequence of the high torus-plenum conductance and hence a design effort to reduce this conductance is warranted. Table II presents an inventory of T_2 and He gas quantities passed through the major components of the model.

TABLE II

QUANTITY OF T_2 AND He TRANSFERRED THROUGH SELECTED COMPONENTS OF THE TANGENTIAL CHARGE EXCHANGE VACUUM MODEL

Gas Species	Component	Torr·ℓ	Curies
T_2	Torus Gas Feed	100	340
	Fore Plenum Pump	1.6	5.5
	Analyzer*	3.6×10^{-4}	1.2×10^{-3}
		0.9×10^{-4}**	0.3×10^{-3}**
He	Cell Gas Feed*	4.0×10^{-3}	—
	Fore Plenum Pump	1.7×10^{-4}	—
	Torus (Total)	5.8×10^{-5}	—

*For each analyzer module.

**Analyzer valve closed after plasma discharge.

VI. ANALYSIS OF THE DIAGNOSTIC NEUTRAL BEAM VACUUM SYSTEM

The diagnostic beam serves to enhance the charge exchange production from a localized region defined by the intersection of the beam with the viewing field of a

given analyzer. This enhancement both improves the signal level and as well provides spatial resolution for the charge exchange measurement. As indicated in Fig. 1 and Fig. 2, the beamline can be moved about a pivot point, thus allowing the beam to be steered across the viewing field of either the perpendicular or tangential analyzer systems.

Previous calculations demonstrated that for optimal diagnostic effectiveness over the anticipated range of plasma density for TFTR, the neutral beam should provide hydrogen (and deuterium) species having energies selectable from 20-80 keV with approximately 15 A of total extracted source ion current. This results in a megawatt-like power level which leads to a requirement for cryogenic pumping of the beamline to handle the associated ion source gas loads. The conceptual isometric diagram of the beam system shown in Fig. 3 illustrates the layout of the major components in the system. Hydrogen (or deuterium) gas feeds an ion source which produces a beam of singly charged ions with components at the full, half, and one-third fractional energies of the chosen source extraction potential. After emerging from the neutralizer cell, a deflection magnet deposits the residual ions on an ion dump while the energetic neutrals pass through beam shaping apertures and a drift duct into the torus. Retractable copper plate calorimeters serve to measure the neutral beam power and to control the vertical and horizontal dimensions of the injected beam cross section. The beamline tank is provided with an apertured partition to aid in localizing gas from the ion source. Cryo-panels are located on both sides of the partition to provide differential pumping. This arrangement is effective in reducing the gas pressure in the drift duct and consequently both the loss of neutral beam power due to reionization as well as flow of the source gas into the torus.

The nodal network used to model the diagnostic neutral beam vacuum system is shown in Fig. 20. Of the 200,000 ℓ/s LHe cryo-pump capacity, 3/4 is allocated to

the corresponding fraction of the beamline tank containing the neutralizer and ion magnet/dump. The remaining 1/4 provides pumping for the calorimeter chamber and the drift duct. The duct is provided with two valves; one near the torus to isolate the beamline/duct for maintenance purposes and the other near the beamline to limit torus/source gas exchange during beam operation.

Certain approximations used in modeling the cryo-condensing pumps require explanation. These pumps are usually operated in the molecular flow pressure range and the pump speed is generally constant versus pressure until the partial pressure of the pumped gas approaches the vapor pressure of that gas at the cryo-panel temperature. The pump speed depends on the gas molecular weight. In the absence of test data, the model approximates the speed ratio for two gases having different molecular weights, M, by $S_1/S_2 = (M_2/M_1)^{1/2}$. The constant speed values from the input data table are automatically reduced within the VSTS program as the partial pressure of a specie approaches the vapor pressure limit at the temperature of the condensing panel. Corrected speed is determined from $S_c = FS_t$ where S_t is the tabulated pump speed and F is the vapor pressure limit correction factor determined from

$$F = 1 - \frac{P_v}{P}\left(\frac{T_{CHEV}}{T_{CP}}\right)^{1/2} .$$

Here P_v is the vapor pressure of the specie at the panel temperature, T_{CP}, the temperature of the chevron in front of the panel is T_{CHEV} (usually LN_2 at 77°K), and P is the partial pressure of the specie being pumped. Two approximations made in the VSTS cryo-pump model are noted. First, the specie partial pressure, P, is taken as the pressure existing in the volume being pumped. It is more appropriate, however, to use the partial pressure between the chevron and the condensing panel. Since conductance through the chevron is usually not available in pump specifications, some liberty is taken for model simplification. If actual test data

were available, provision exists in the program to suitably modify the pumping speed performance. Second, the convective and conductive heat transfer between the panel and the chevron in practice modifies the vapor pressure limit. The main consequence of this is that the base pressure produced by the VSTS program is lower by approximately a factor of two than expected in practice.

In operation, the diagnostic neutral beam is required to generate either a single pulse of variable duration up to a maximum of 500 ms or a train of short pulses (~50 ms) over a period of ≤1 sec at a 50% on/off duty cycle. Suitably stringent performance requirements on the vacuum model are imposed by choice of a 500 ms continuous pulse operation. In Fig. 21, the T_2 and H_2 partial pressure transients for the pulsed plasma/beam mode are shown at noted nodal points corresponding to the model of Fig. 20. The tritium transients show the pre-fill and discharge sequence described earlier. Closure of the duct isolation valve is initiated at 3.5 sec and completed 2.5 sec later, after which rapid pumpdown of the duct/beamline ensues due to the large cryo-pump speed. This scenario remains the same for various beam operating changes to be described below. The H_2 transients in Fig. 21 correspond to a 500 ms beam pulse with an ion source gas flow rate of 10 Torr·ℓ/sec. The T_2 and H_2 pressure distributions throughout the beam system are shown in Fig. 22. The shaded region for the H_2 curve represents the pressure excursion under ion source flow rate variation from 5-15 Torr·ℓ/sec. It should be noted that the curve shapes presented in this figure reflect some artistic liberties based on the geometry of the vacuum system.

The following salient features of the beamline vacuum system performance merit comment. In accordance with accepted diagnostic neutral beam design requirements, the neutralizer/source pressure is in the 10^{-2} - 10^{-3} Torr range, the beamline section containing the deflection magnet/neutralizer is $\sim 10^{-4}$ Torr and in the remainder of the system, the H_2 pressure is a few 10^{-5} Torr or less. This

overview remains valid even if the calculated pressures are increased by a factor of two due to the approximations used in the cryo-pump model discussed earlier.

An inventory of the T_2 and H_2 integrated gas flows is given in Table III. The relatively large conductance and slow valve closure associated with the duct results in several Curies of tritium entering the beam chamber, most of this being pumped by the first chamber cryo-panel. The quantity of H_2 entering the torus ($\leq$0.04 Torr·ℓ) corresponds to a partial pressure in the torus of 4×10^{-7} Torr for a torus volume of 10^5 liters. Approximately 95% of the ion source gas load is pumped by cryo-panel 2 situated in the neutralizer/magnet section of the beamline chamber.

TABLE III

QUANTITY OF T_2 AND H_2 TRANSFERRED THROUGH SELECTED COMPONENTS OF THE DIAGNOSTIC NEUTRAL BEAM VACUUM MODEL

Gas Species	Component	Torr·ℓ	Curies
T_2	Torus Gas Feed	100	340
	Duct	0.79	2.68
	Cryo-Panel 1	0.78	2.65
	Cryo-Panel 2	0.01	0.03
H_2	Source Gas Feed (0.5 sec pulse)	5.00	—
	Cryo-Panel 1	4.82	—
	Cryo-Panel 2	0.14	—
	Duct	0.04	—

Cryo-panel operation involves a rather complex, time-consuming start up procedure and, in addition, is relatively expensive to run compared with other vacuum pumps. For these reasons, it is of interest to examine the possibility of operating the diagnostic beam in a short-pulse mode without the use of cryo-pumping. In the short-pulse mode, expansion of the ion source gas load into the 2.8×10^3 liter volume of the

beamline chamber maintains the beamline pressure distribution within acceptable operating values for some period of time. To determine this time, the pressure transients were examined for a 100 ms beam pulse with the cryo-panels inoperative. From the results shown in Fig. 23, it can be seen that the beamline H_2 pressures approach the acceptable operating limits near the end of the 100 ms pulse. It is concluded, therefore, that beamline operation without cryo-pumping (using volume expansion) is viable for pulse lengths not exceeding ~100 ms. For pulse lengths near 100 ms, some droop in neutral beam power should be anticipated due to reionization losses.

VII. DISCUSSION

In this section, an overview of the salient aspects of the preceding vacuum system analyses is presented and some additional observations are discussed.

For the perpendicular charge exchange vacuum system, use of a pumped plenum between the analyzer/torus chambers and a low conductance restriction near the analyzer are essential to achieve the required vacuum system performance. Each analyzer requires a net effective pumping speed for He of approximately 800 ℓ/s. Unfortunately, the turbomolecular pumps commercially available at the present time are either ~50% larger than needed, or ~50% smaller. Through careful design of the stripping cell, reduction of the He gas load appears feasible which would permit use of the smaller, less expensive turbomolecular pumps (for example, 500 ℓ/s Leybold-Heraeus). Resolution of this point is expected to derive from evaluation of a prototype analyzer module which is in progress. The exchange of working gases between the torus and analyzers is well within acceptable design values. Most of the preceding remarks apply equally to the tangential charge exchange system. However, the large aperture between the plenum and the torus stemming from the viewing field requirements of this analyzer system poses a special problem. With a simple

adequately large-area clear aperture, the tritium transfer to the analyzer system is marginally acceptable for TFTR operation at maximum tritium loading. A design effort to reduce the conductance of the aperture/torus interface is recommended. With the exception of the tangential vacuum plenum, the tritium pumped through the analyzer components of both charge exchange systems is 10^{-5} - 10^{-8} times less than the maximum tritium load handled by the main torus vacuum system. This poses the as yet unresolved question as to whether or not specially modified turbomolecular pumps with all-metal vacuum-to-atmosphere seals are required for the analyzer vacuum system.

The cryo-pumped diagnostic neutral beam system meets or exceeds all of the vacuum design requirements both for proper beam operation as well as torus interface vacuum considerations. In addition, the vacuum analysis indicates that short-pulse (≤ 100 ms) beam system operation is feasible without use of cryo-pumping by utilizing expansion of the ion source gas load in the large volume provided by the beamline chamber.

The emphasis of this report has been on evaluation of the performance of the charge exchange diagnostic vacuum systems and the interchange of torus/diagnostic working gases. A further consideration is the influence of the charge exchange systems on the TFTR discharge scenario. Specifically, following an initial gas pre-fill phase, the torus continues to be fed with gas at a programmed rate throughout most of the discharge duration. The diagnostic vacuum connections become loaded with some quantity of gas during the prefill stage. Part of this gas load re-enters the torus during the discharge and thus impacts on the total gas feed rate to the torus. An estimate of the gas re-entering the torus from the diagnostic system can be obtained from the VSTS flow rate transients over the duration of the discharge for the appropriate ducts connecting to the torus. The results are given in Table IV. For these calculations, the tritium gas feed rate to the torus was constant throughout the

discharge pulse at 100 Torr·ℓ/sec. The total tritium re-entry rate from the charge exchange diagnostic systems is estimated at 1.3×10^{-1} Torr·ℓ/sec. The tritium re-entry for the complete analyzer system is $\lesssim$0.2% of the quoted torus feed rate and would appear to be negligible. However, the same conclusion may not be valid when all connections to the torus are accounted for and smaller gas feed rates during the discharge are used.

TABLE IV

INVENTORY OF TRITIUM RE-ENTRY TO THE TORUS
FROM THE PRE-FILL LOADED DIAGNOSTIC CONNECTIONS

Diagnostic System	Average Tritium Re-entry Flow Rate (Torr·ℓ/sec)
Perpendicular Charge Exchange	
1 Arm (400 cm long, 5.72 cm diameter tube)	3.0×10^{-4}
12 Arms	3.6×10^{-3}
Tangential Charge Exchange	8.0×10^{-2}
Diagnostic Neutral Beam	5.0×10^{-2}

ACKNOWLEDGMENTS

The author gratefully acknowledges the encouragement and support of Ken Young and Myron Norris in initiating this project, and the expert work of Herb Fishman in adapting the VSTS program to the PPLCC CYBER computer. Discussions with Remo Campanile, Sam Goldfarb, Rob Goldston and George Martin led to numerous contributions to the vacuum design in which the author expresses his appreciation. Special recognition is extended to Joe Sredniawski for making the VSTS computer program available and accelerating my learning curve in the present application.

This work was supported by the U. S. Department of Energy under Contract No. EY-76-C-02-3073.

REFERENCES

1. Sredniawski, J., "Vacuum System Transient Simulator Users' Manual," Tokamak Fusion Test Reactor Engineering Report No. EP-D-006, 1 Nov 1977.

2. Fishman, H. and Medley, S. S., PPPL Report, in preparation.

3. Malinowski, M. E., "Tritium-Caused Background Currents in Electron Multipliers," Sandia Laboratories Report, SAND79-8218 (May 1979).

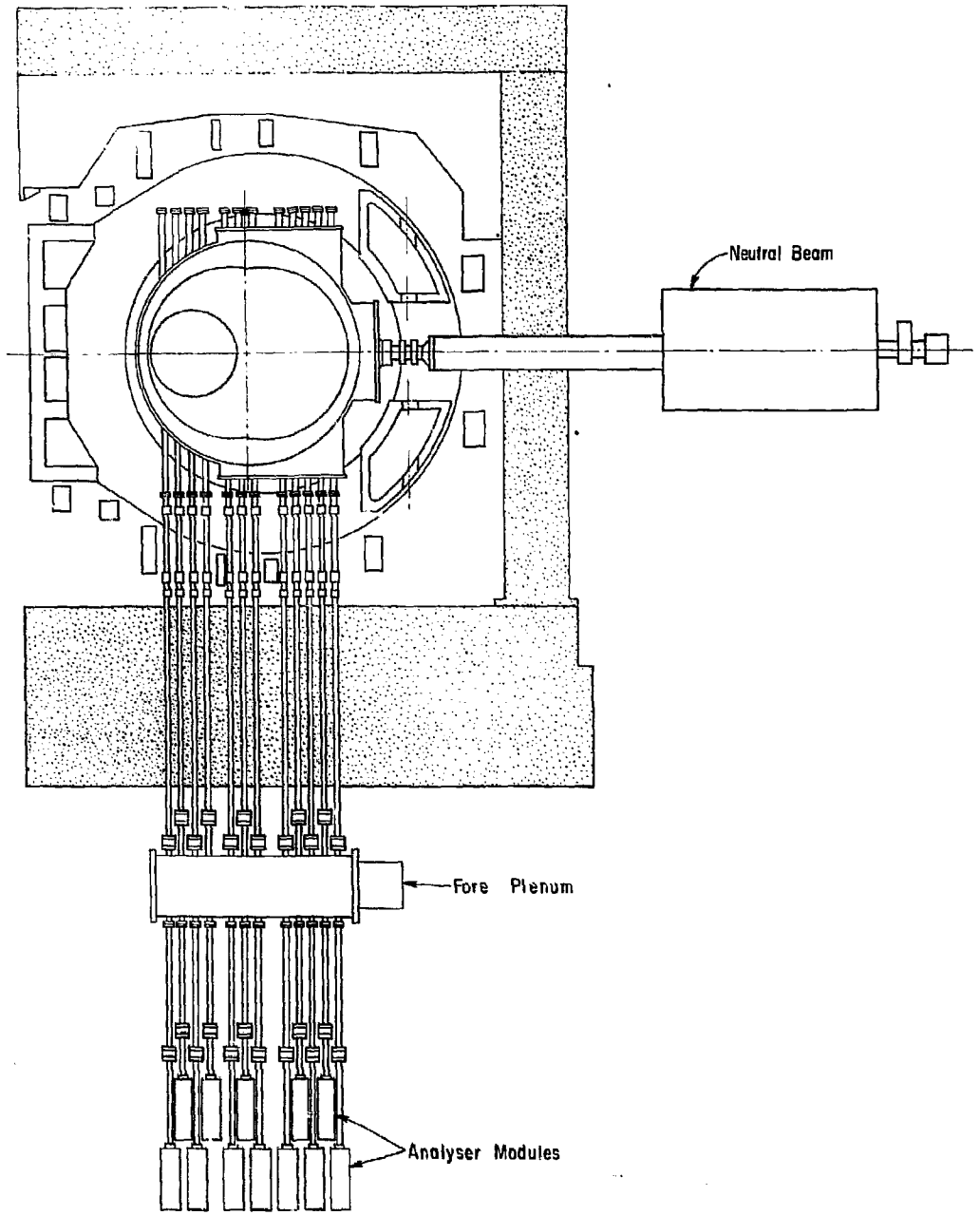

PPPL 793441

Fig. 1. Layout of the TFTR perpendicular charge exchange analyzer system.

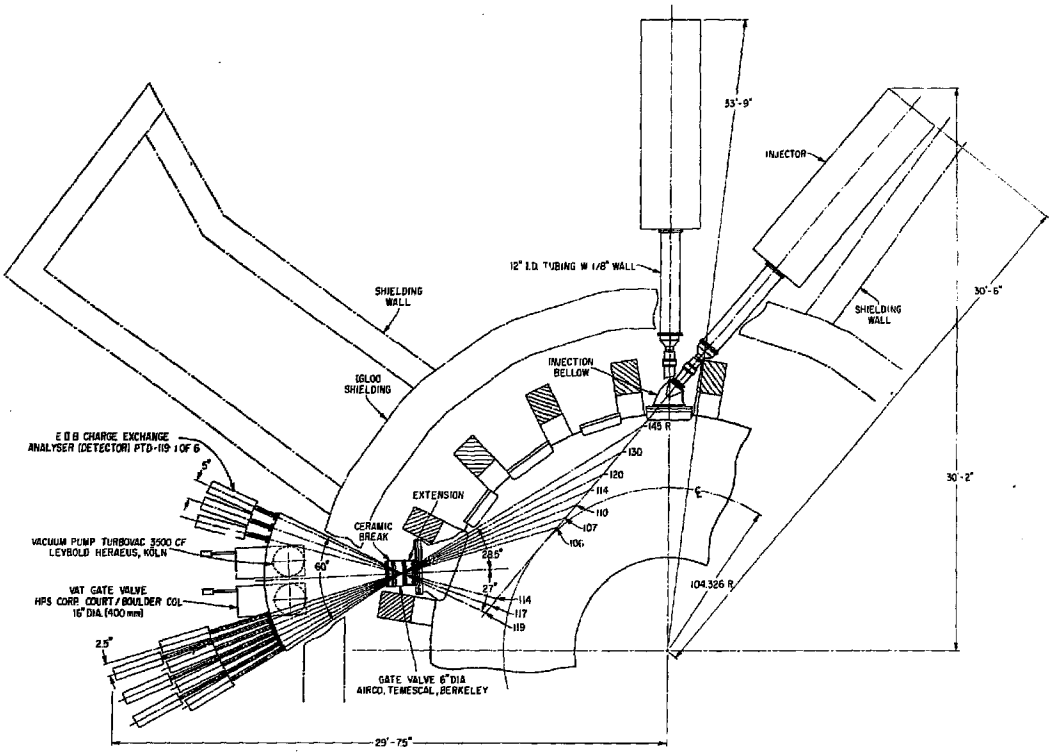

PPPL 783808

Fig. 2. Layout of the TFTR tangential charge exchange analyzer system.

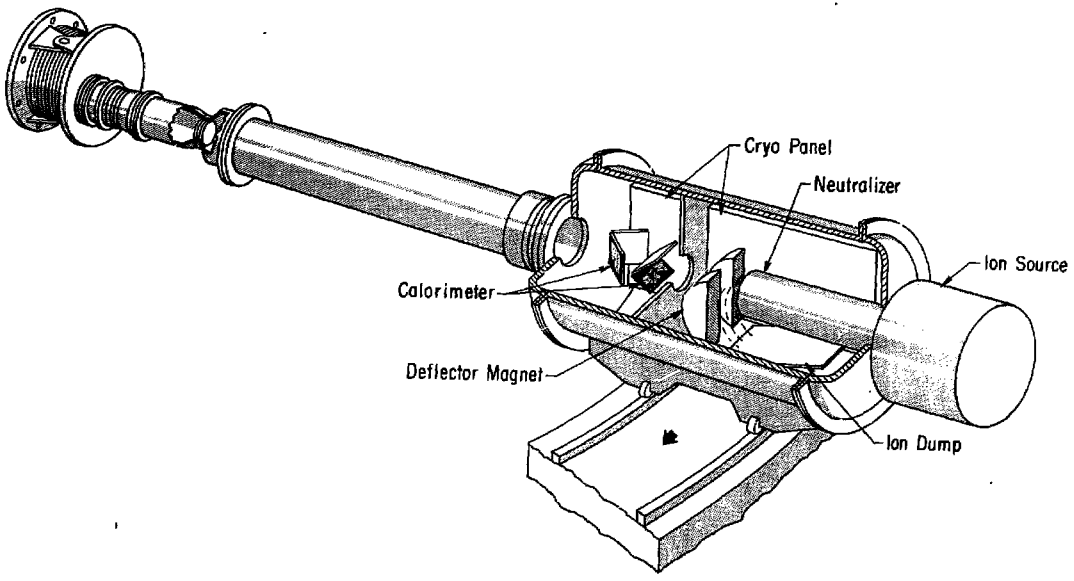

PPPL 793419

Fig. 3. Layout of a conceptual design for the TFTR charge exchange system diagnostic neutral beam.

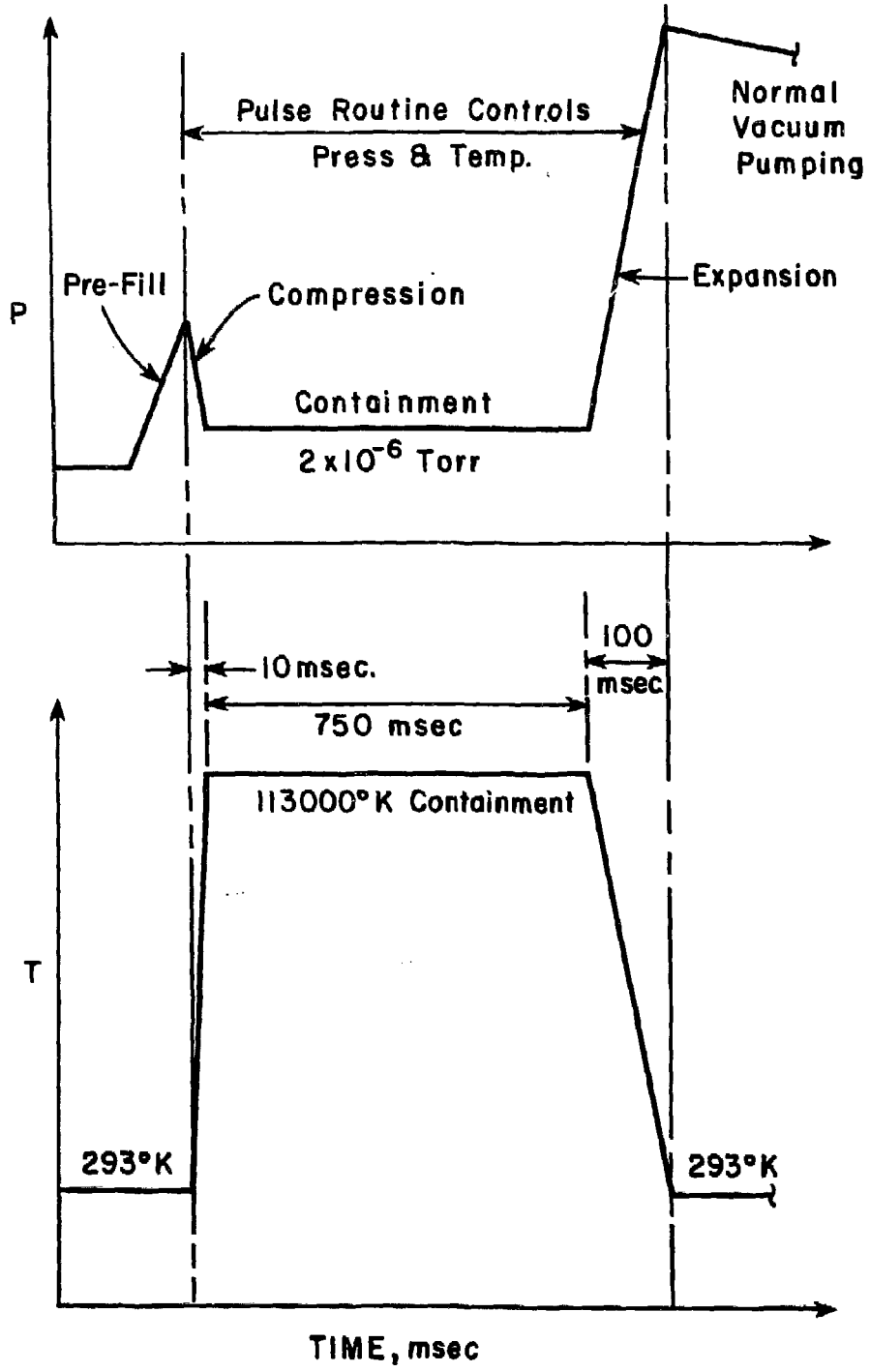

PPPL 793440

Fig. 4. VSTS pulsed routine scenario for TFTR plasma discharge.

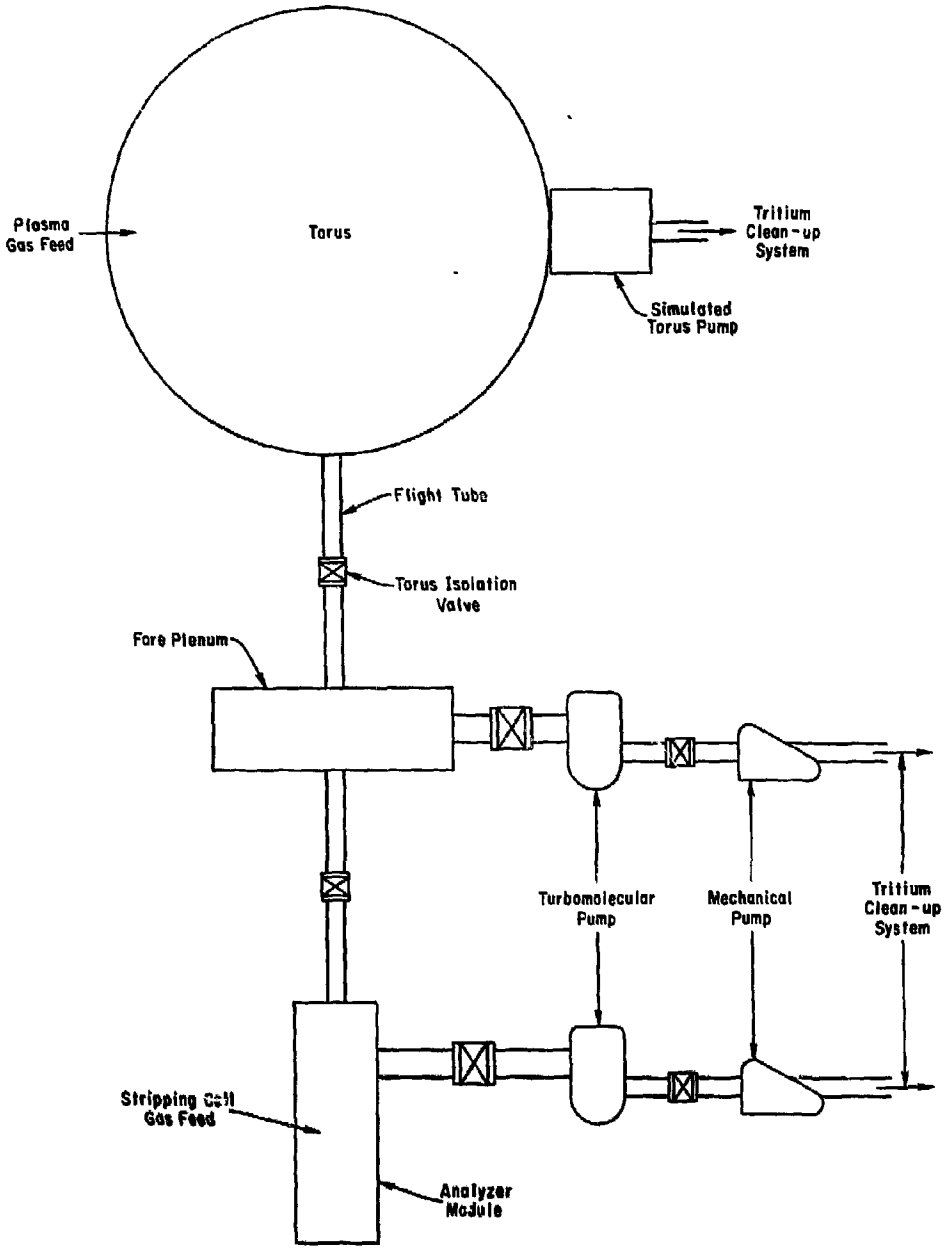

PPPL 793462

Fig. 5. Mechanical schematic for one arm of the perpendicular charge exchange analyzer system.

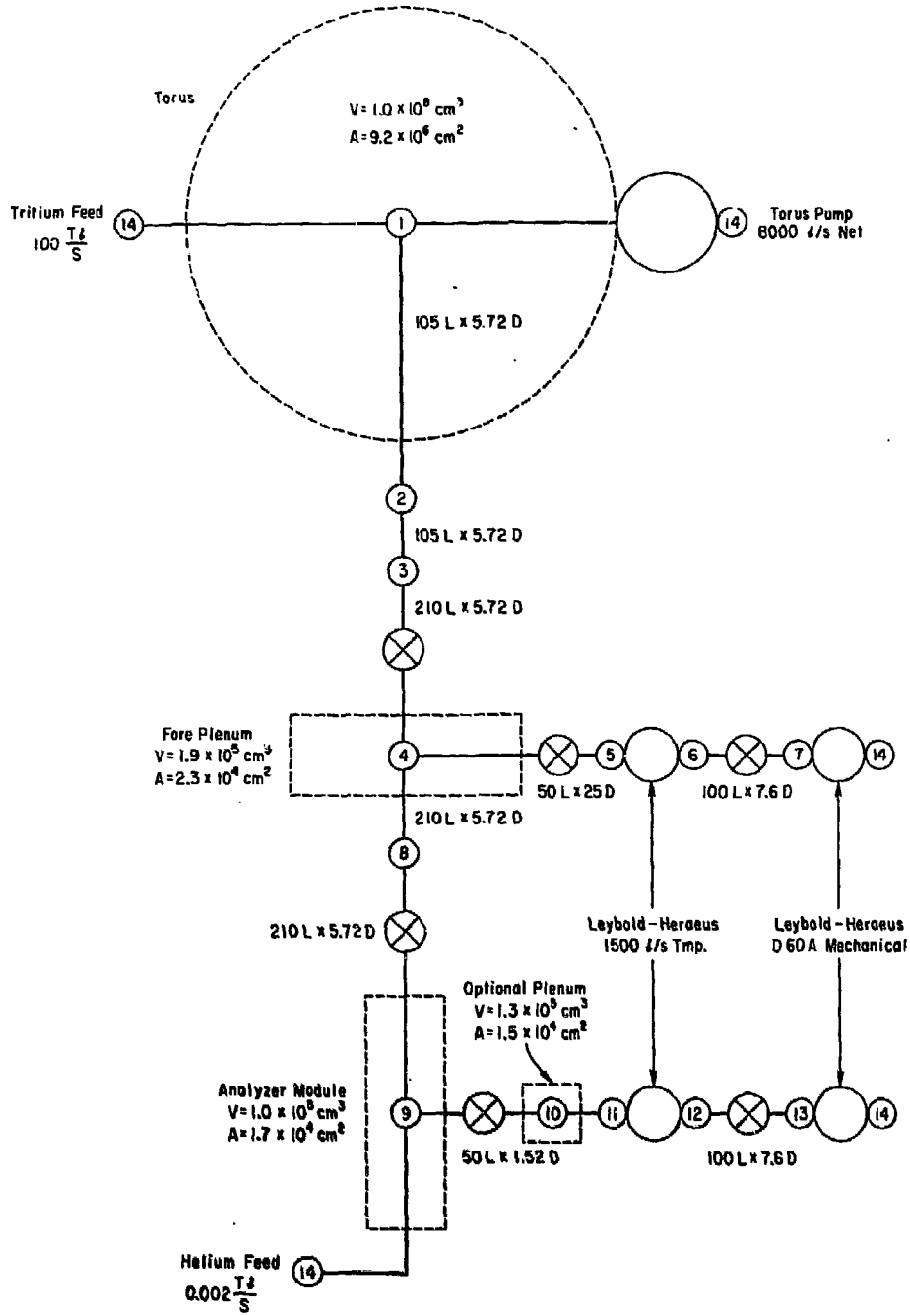

PPPL 793459

Fig. 6. Nodal representation for a single arm of the perpendicular charge exchange vacuum network.

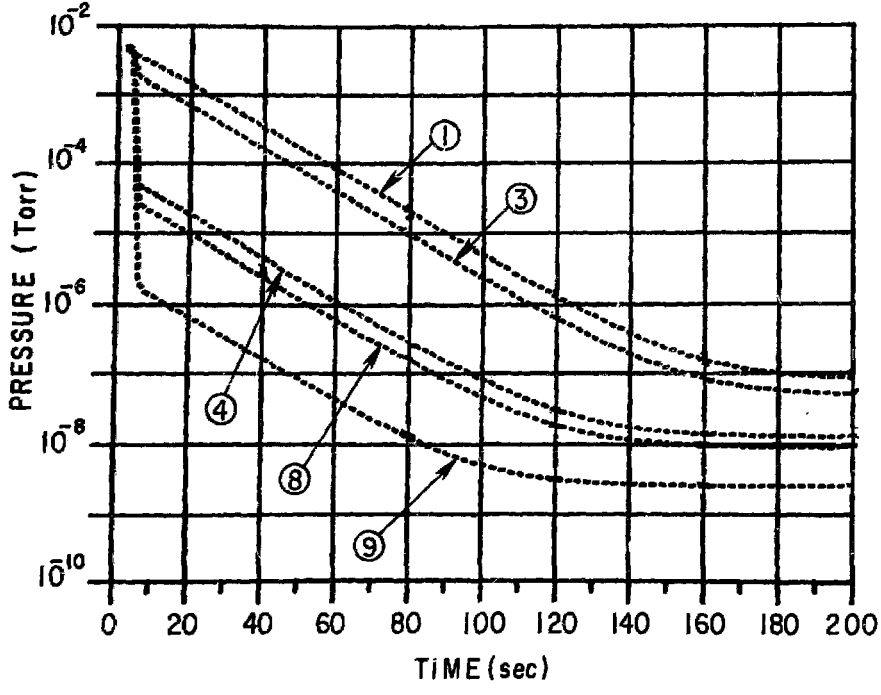

PPPL 793493

Fig. 7. Baseline performance characteristics of the torus/analyzer vacuum system model.

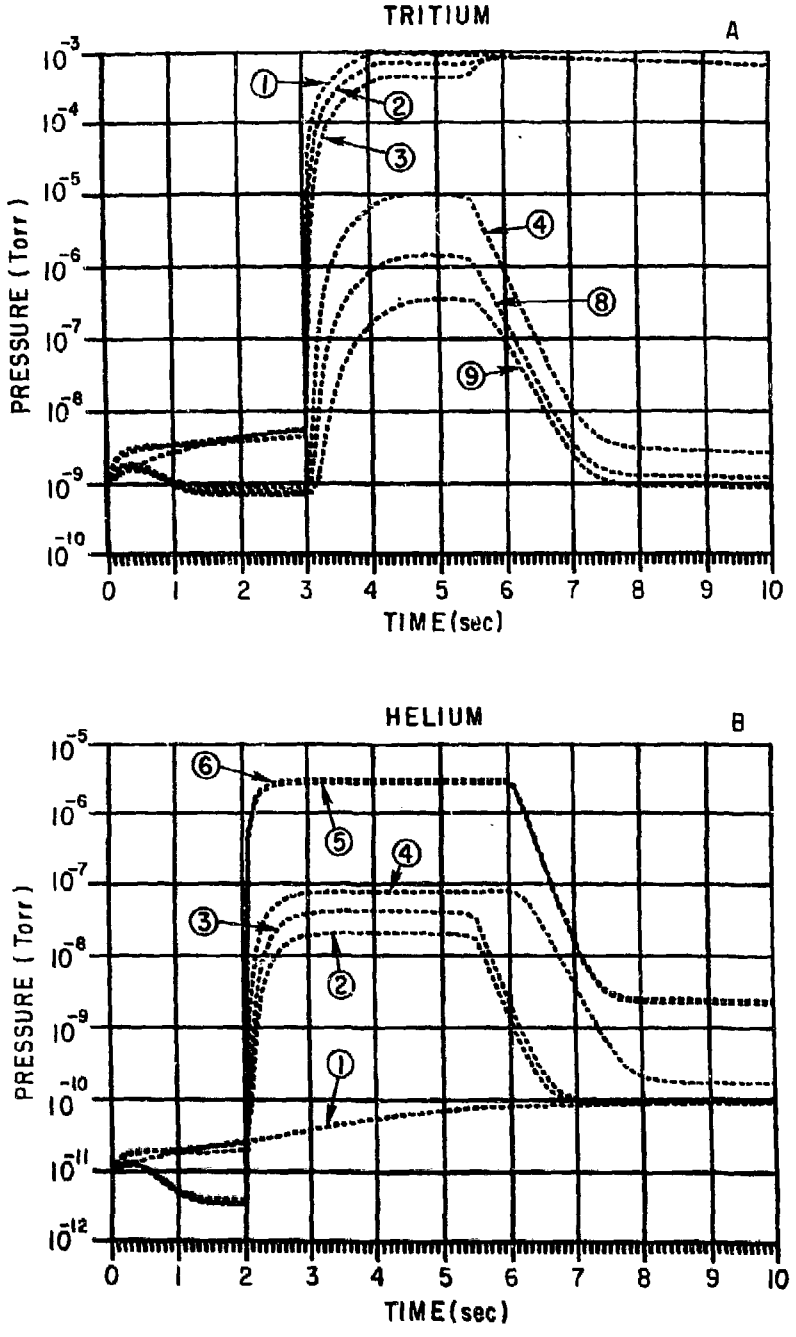

PPPL 793498

Fig. 8. Transient partial pressure distributions for T_2 (A) and He (B) in the single arm model under T_2 and He gas puffing operation.

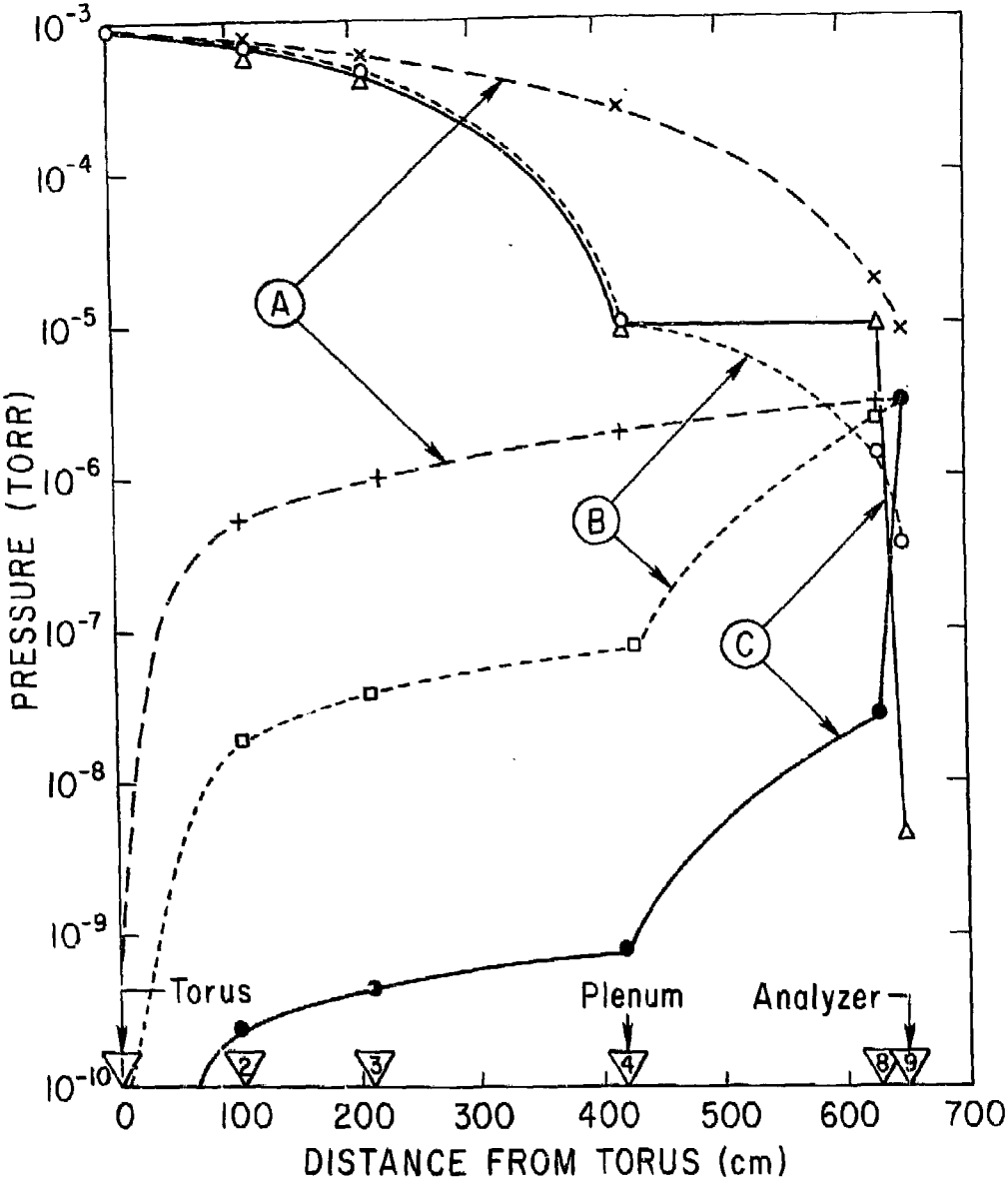

PPPL 793420

Fig. 9. Pressure distribution (t = 5.0 sec) as a function of nodal location from the torus to the analyzer for several network variations (see text).

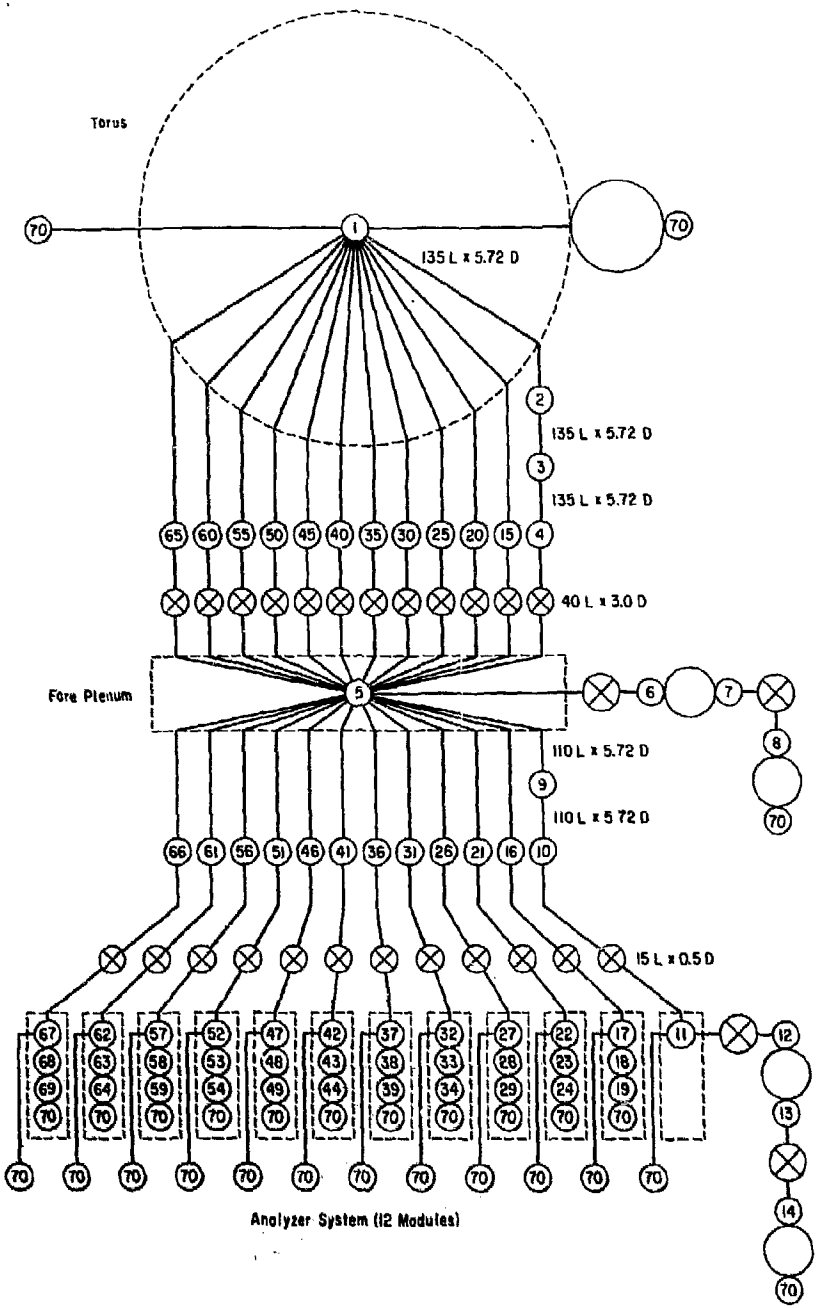

PPPL 793460

Fig. 10. Nodal network for the complete perpendicular charge exchange vacuum system.

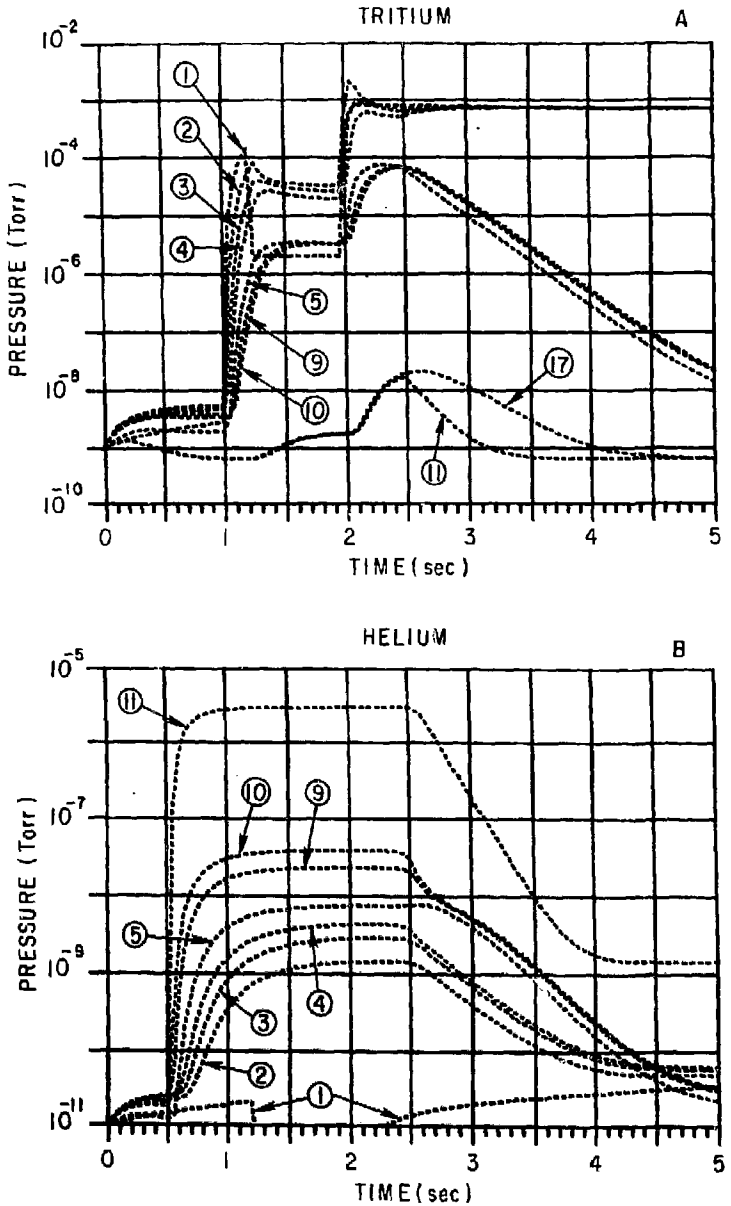

PPPL 793499

Fig. 11. T_2 (A) and He (B) partial pressure transient curves for the perpendicular charge exchange vacuum system model using the plasma discharge simulation mode.

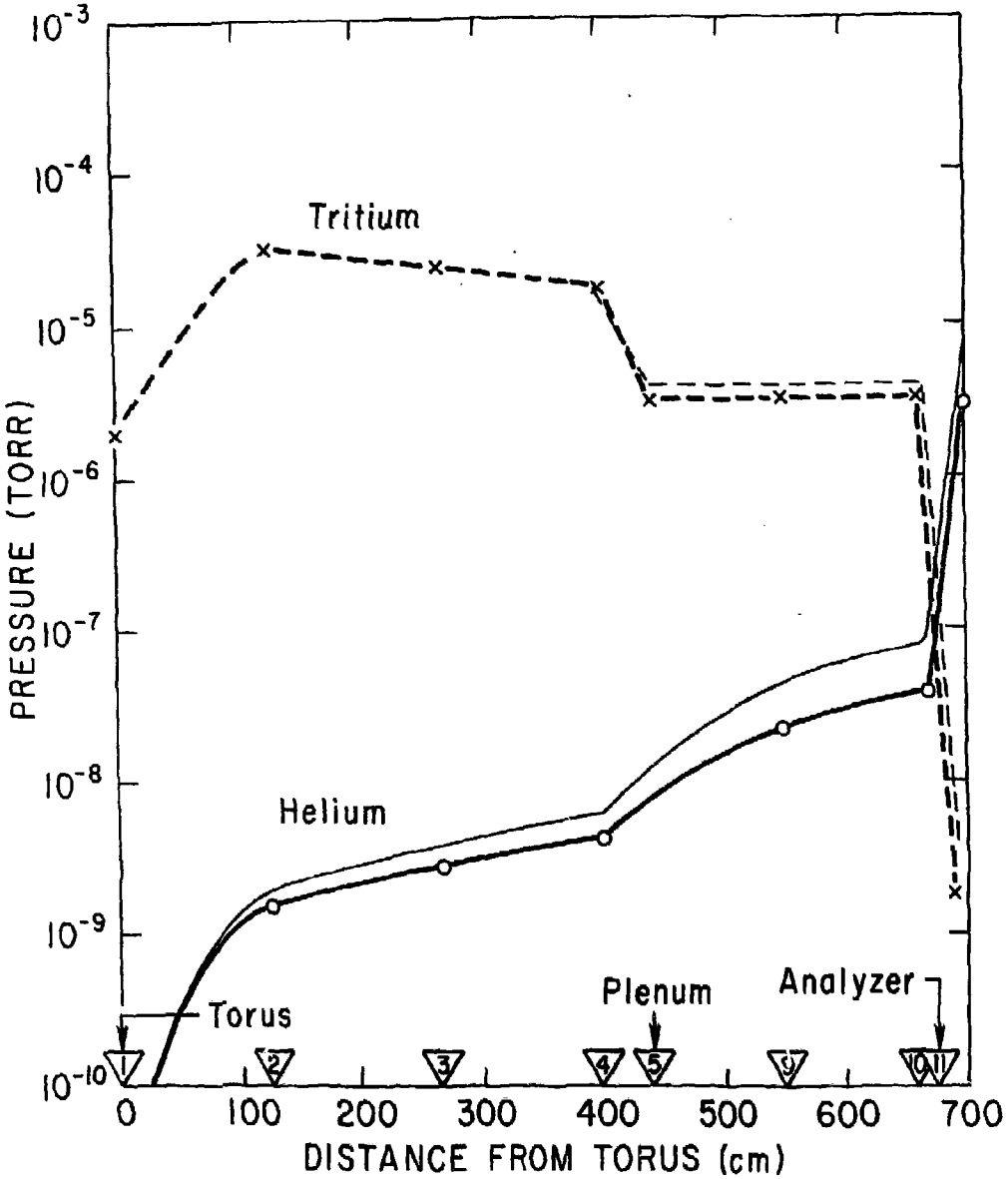

PPPL 793421

Fig. 12. T_2 and He partial pressure distributions (t = 1.9 sec) as a function of distance between the torus and analyzer modules.

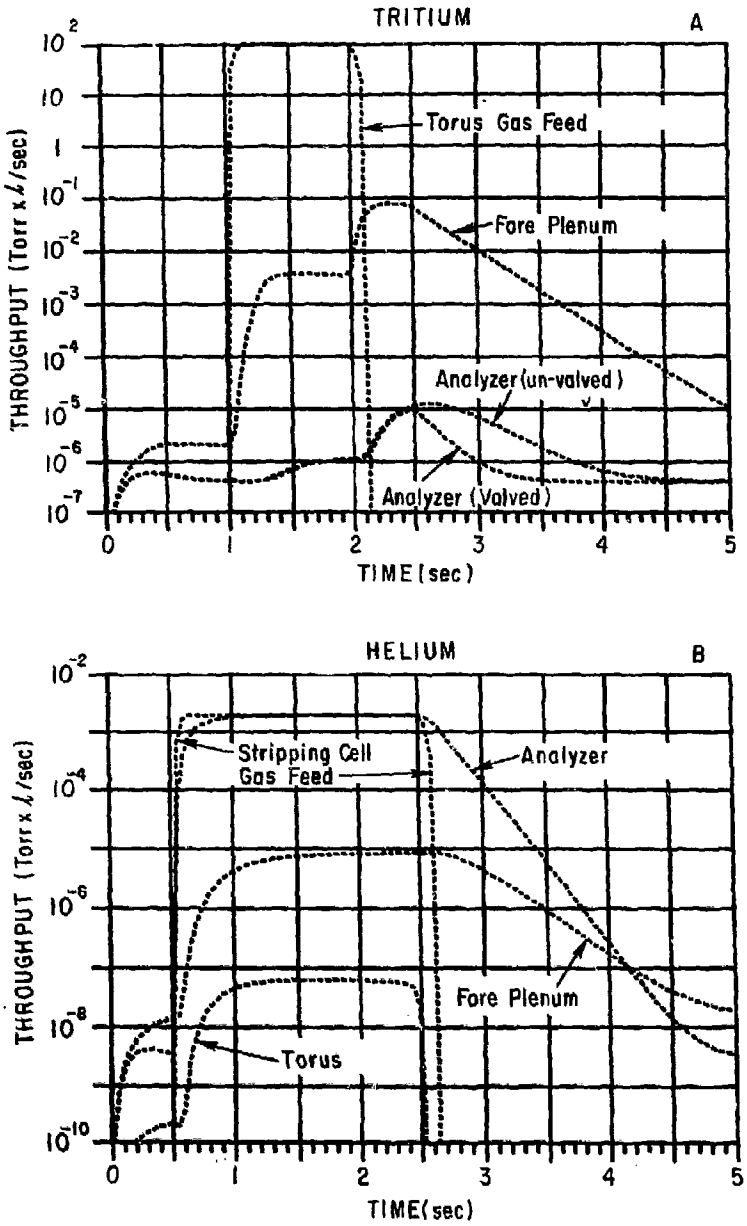

PPPL 793494

Fig. 13. Throughput of T_2 and He for selected components in the perpendicular charge exchange model as a function of time.

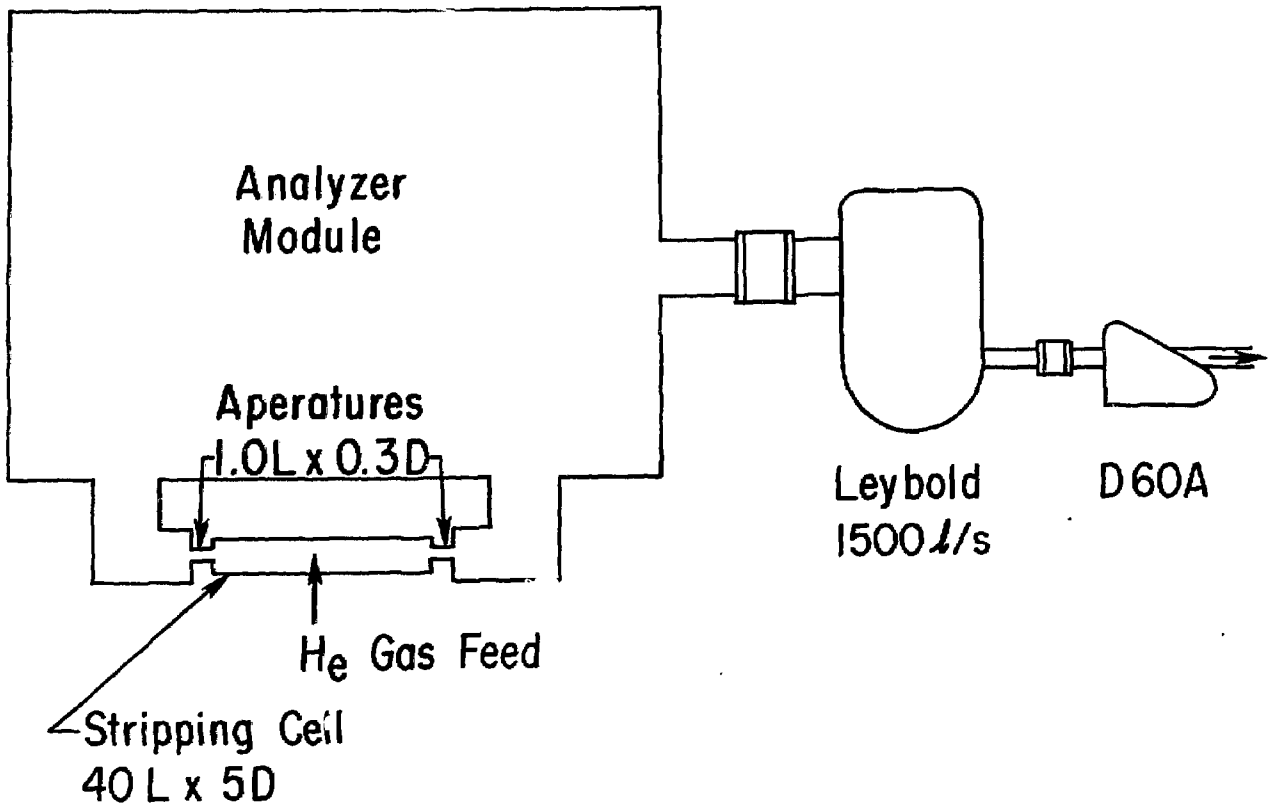

PPPL 793500

Fig. 14. Mechanical layout for stripping cell model.

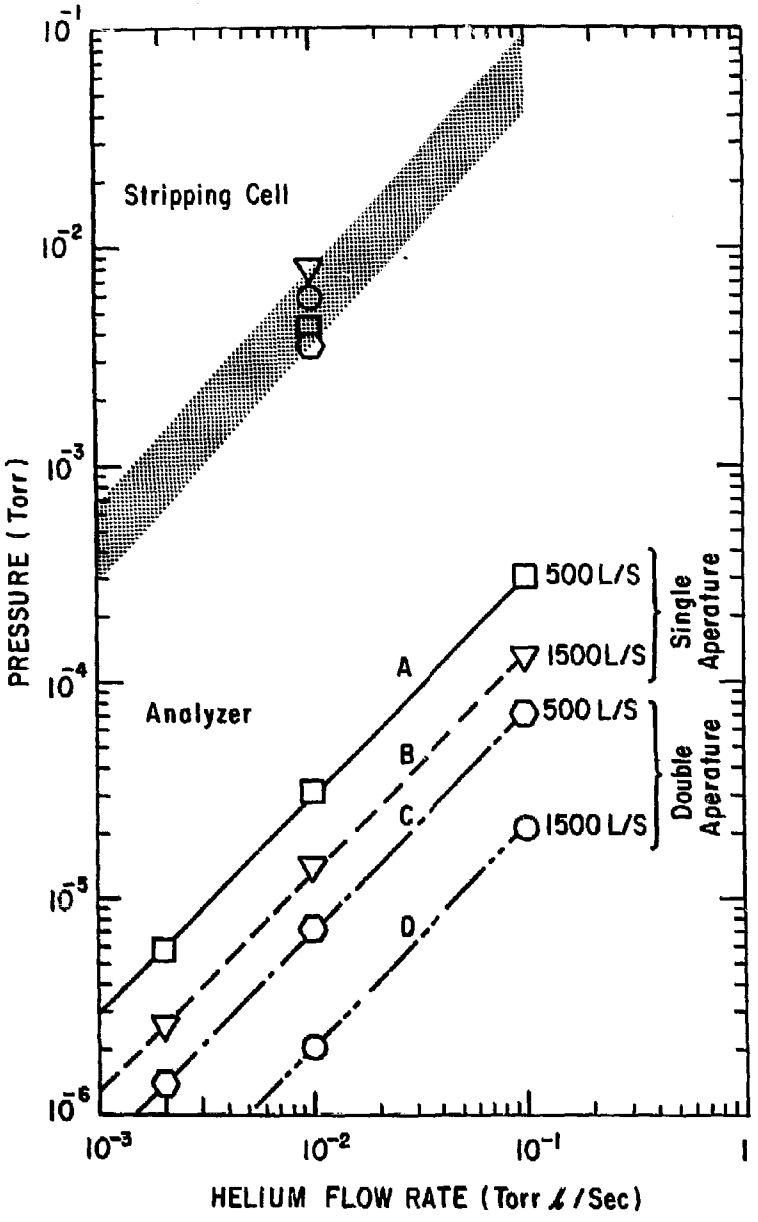

PPPL 793504

Fig. 15. Stripping cell and analyzer pressure as a function of helium flow rate for selected pump and cell aperture configurations.

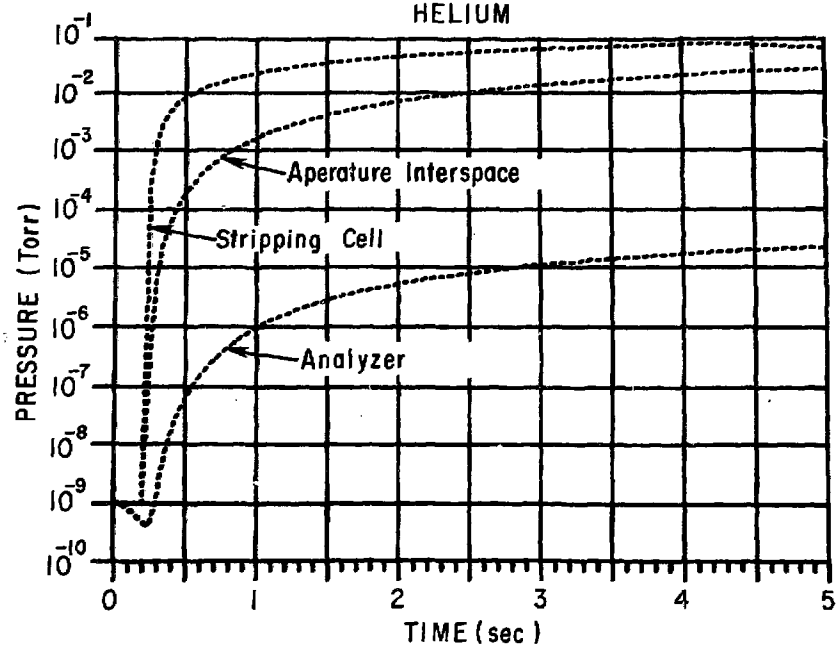

PPPL 793491

Fig. 16. Helium pressure transients for the double aperture stripping cell arrangement.

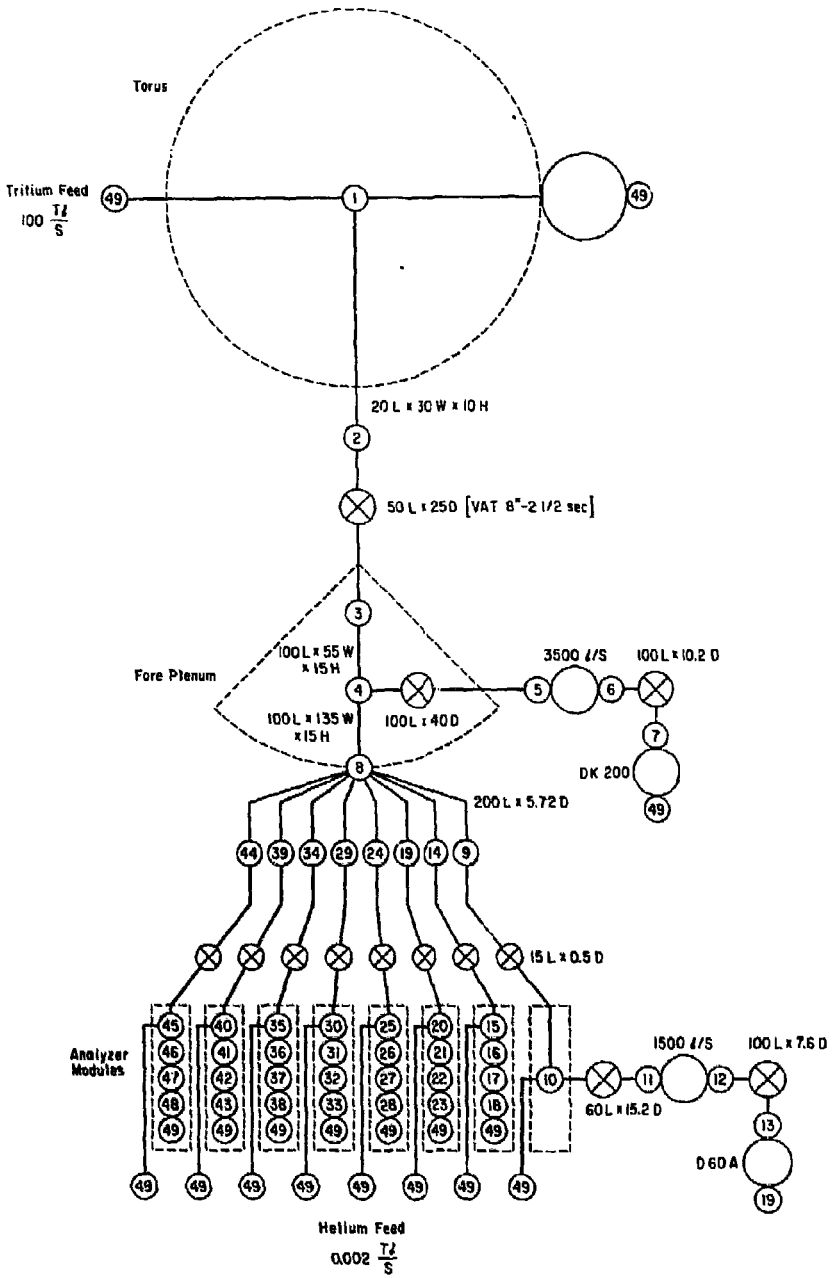

Fig. 17. Nodal network for the tangential charge exchange system.

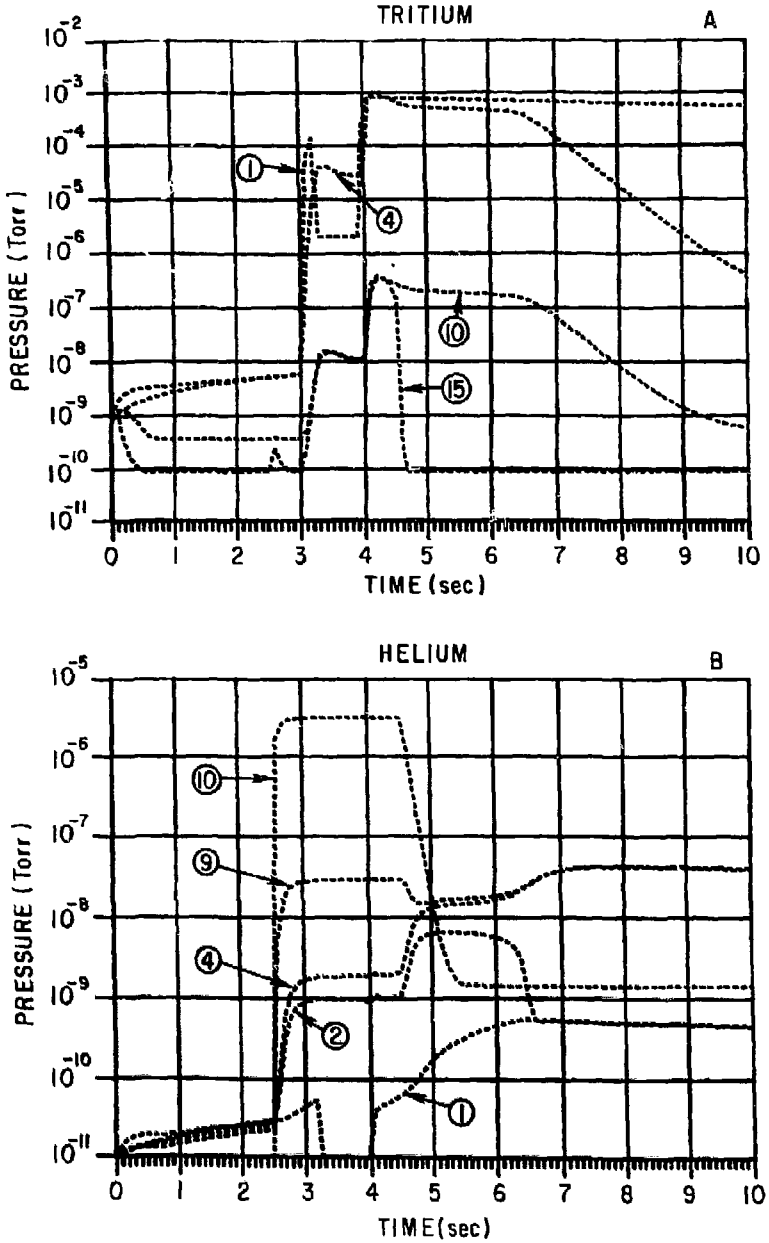

PPPL 793496

Fig. 18. T_2 (A) and He (B) pulsed discharge partial pressure transients for the tangential vacuum system model.

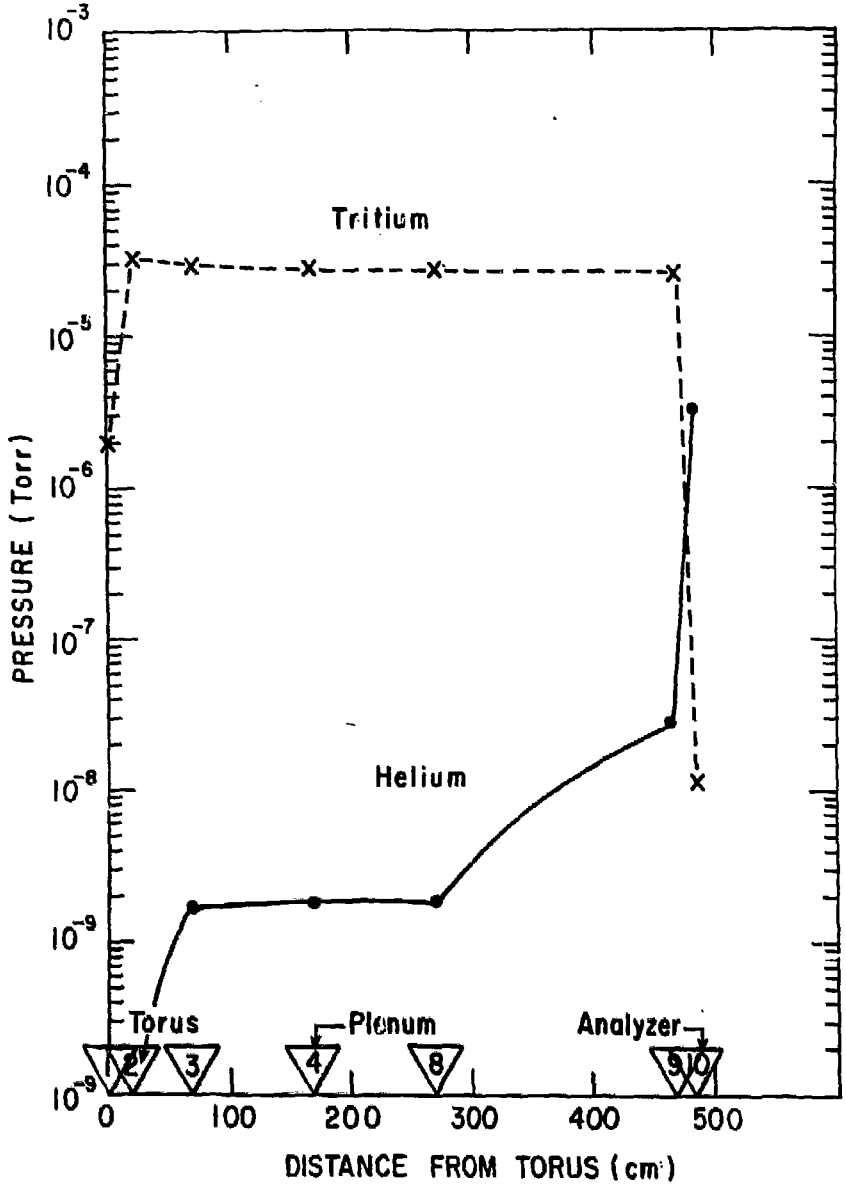

PPPL 793502

Fig. 19. T_2 and He partial pressure distributions during the plasma discharge as a function of distance from the torus.

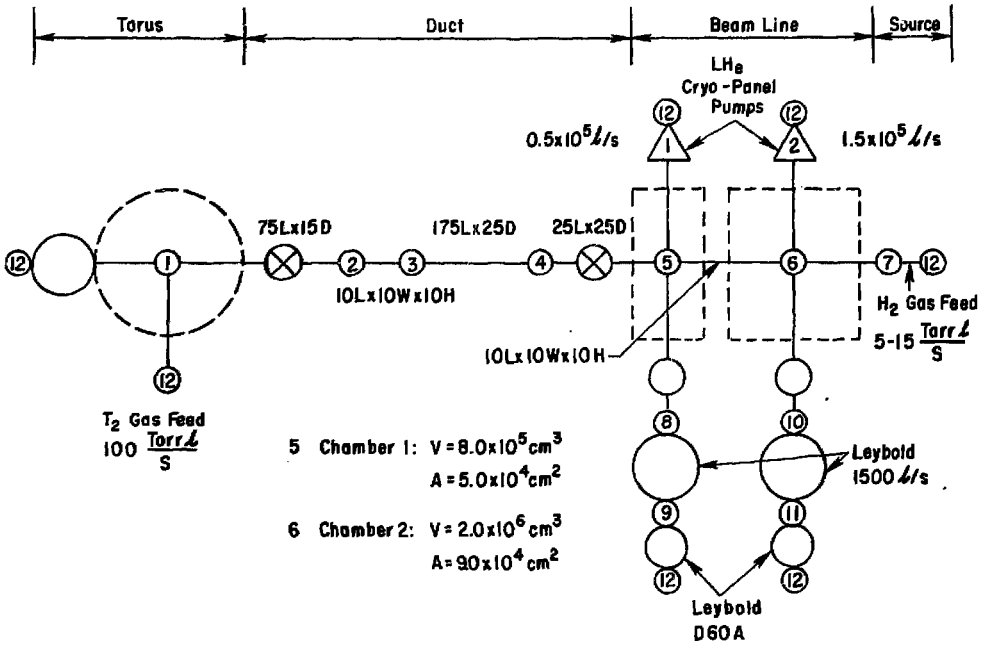

PPPL 793503

Fig. 20. Nodal network for the diagnostic neutral beam vacuum model.

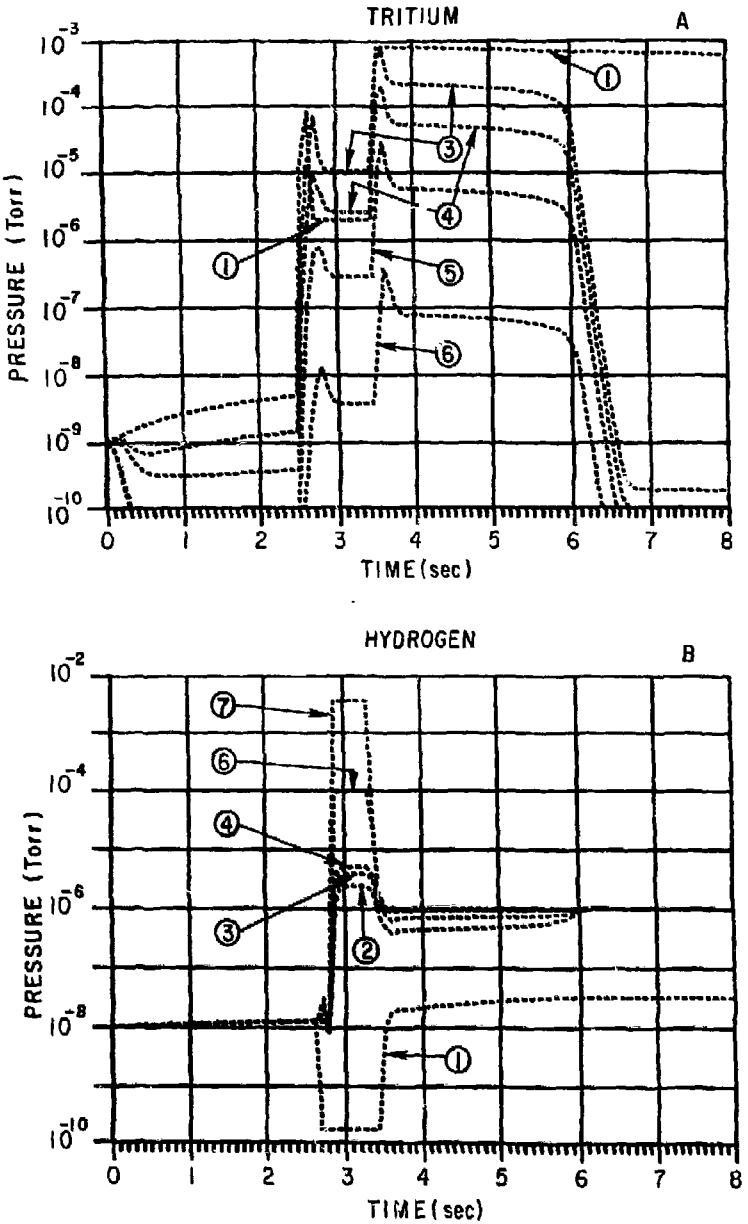

PPPL 793495

Fig. 21. T_2 and H_2 partial pressure transients for the diagnostic neutral beam vacuum system with 10 ℓ/s - H_2 source gas feed.

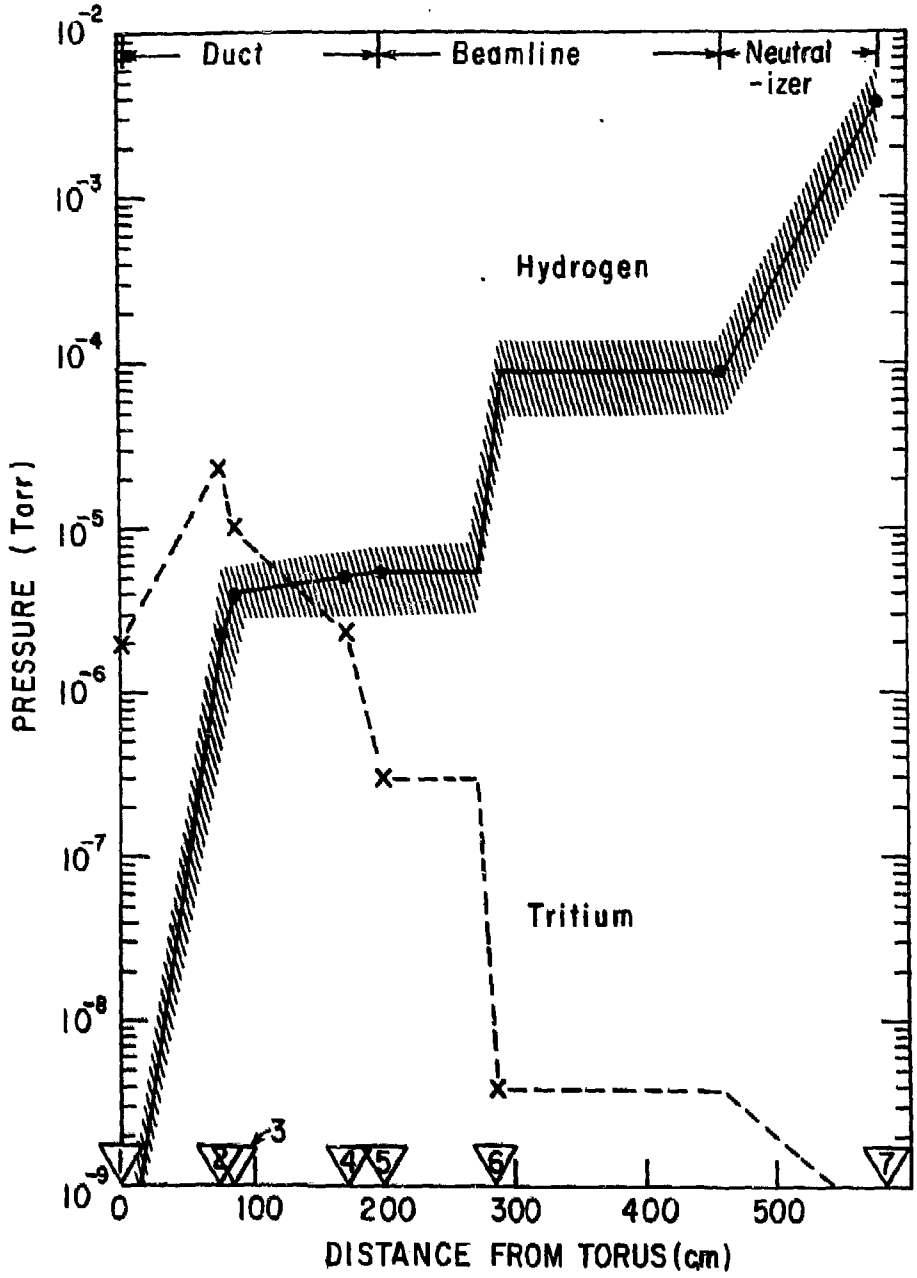

PPPL 793501

Fig. 22. H_2 and He partial pressure distributions during the diagnostic neutral beam pulse as a function of distance from the torus. The shaded region corresponds to the range of hydrogen pressures for 5-15 Torr·ℓ/sec hydrogen source feed rate.

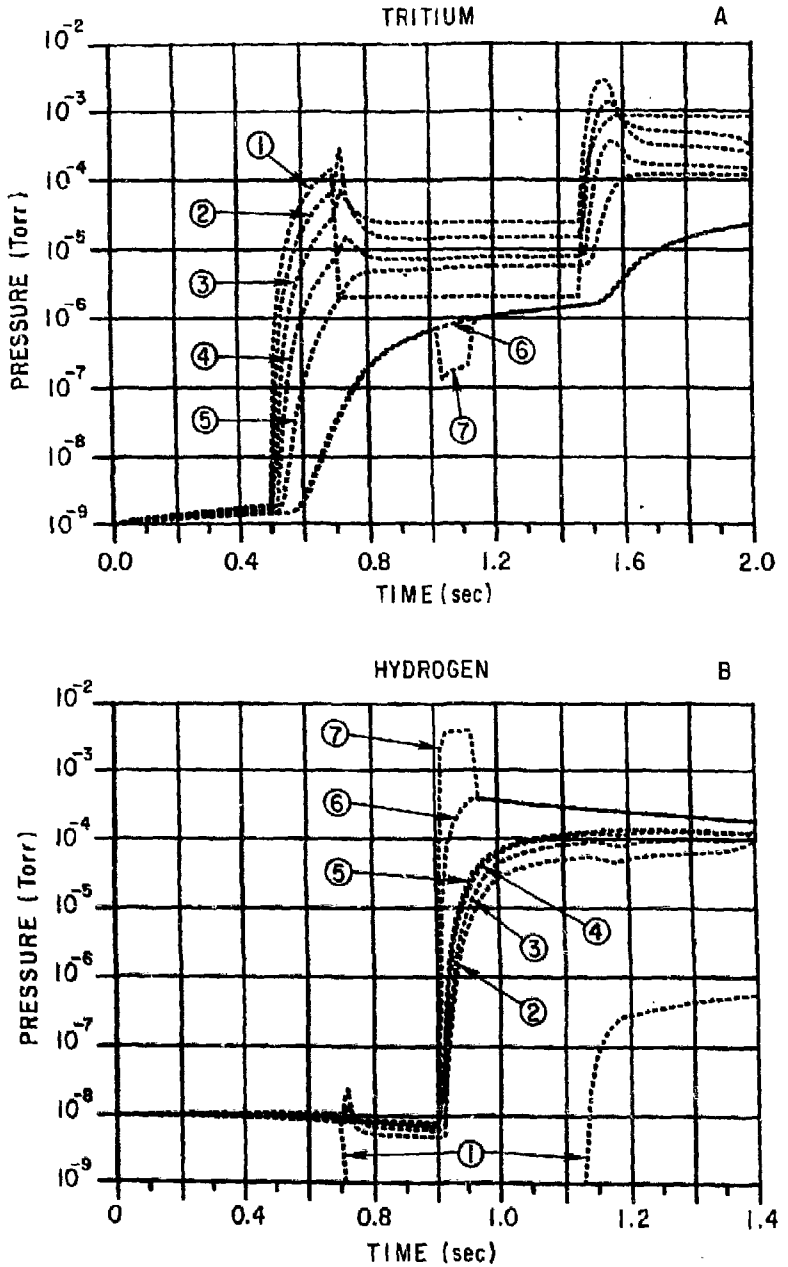

PPPL 793497

Fig. 23. T_2 and H_2 partial pressure transients for short pulse (100 ms) operation of the diagnostic neutral beam using volume expansion without any vacuum pumping (10 ℓ/s H_2 feed rate).